Offline analysis and identification of events in the test run data

Vahe Sokhoyan

TPC Collaboration Meeting
Mainz, 09.03.2020

Institut für Kernphysik

JG|U
JOHANNES GUTENBERG UNIVERSITÄT MAINZ

Cluster of Excellence
PRISMA+
Precision Physics, Fundamental Interactions and Structure of Matter

SFB 1044
THE LOW-ENERGY FRONTIER OF THE STANDARD MODEL

Contents

- Identification of events in the offline analysis
- Analysis of 2017 data (^{4}He in ACTAF2 prototype)
- Analysis of 2019 data (hydrogen in ACTAF2 prototype)
- Investigation of background sources – first steps
- Relation beetween precision, systematics, and radiative corrections
- Summary and outlook

Feasibility and test experiments at MAMI

Segmented anode

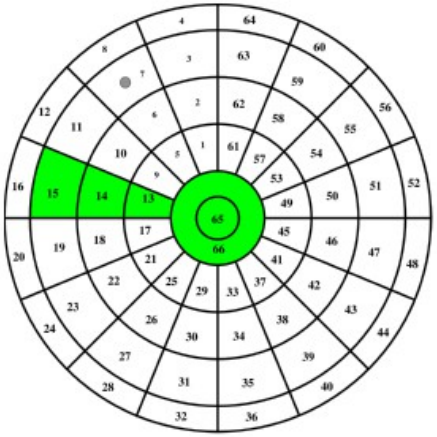

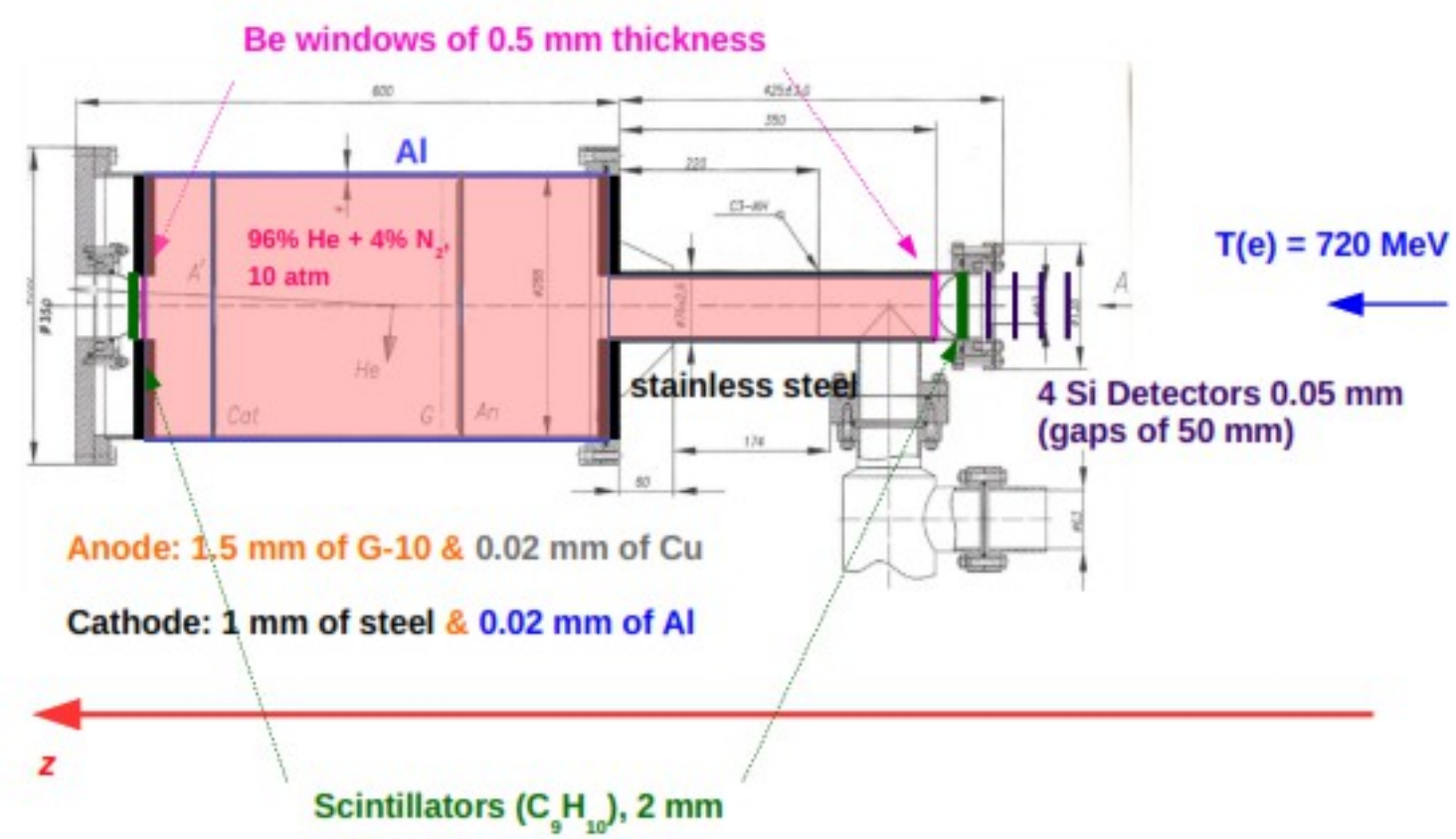

Determination of the optimal run conditions for the main experiment:

- Study of the background created by the electron beam at the intensity of 2×10^6 e/sec
- Development and test of a prototype for a beam monitoring system
- Measurement of the parameters of the low-intensity electron beam at 2×10^6 e/sec, $\sim10^4$ e/sec, and $\sim10^3$ e/sec

→ Identification of events → extraction of cross sections

Conditions of the He test run

- TPC at the electron beamline in the A2 Hall: Helium + 4.3% Nitrogen at 5 and 10 bar
- Upstream and downstream scintillator counters (2mm thick, 55x55 mm) + 4-layer pixel detector (HV-MAPS, 3x3 mm)
- Self triggering mode: Any signal in the anode exceeding 300 keV
- Very low background in the TPC except the central pad

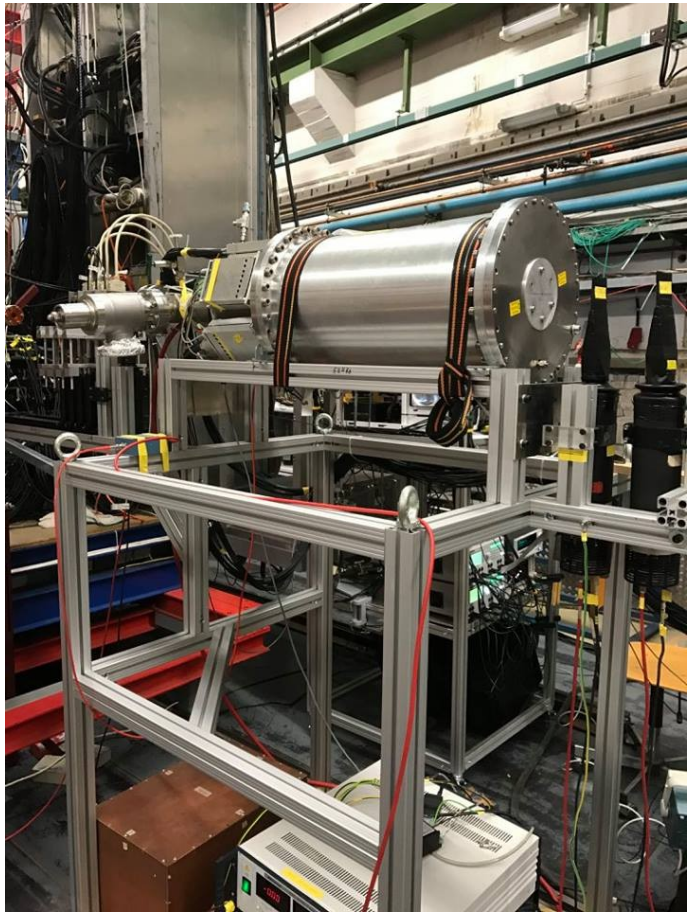

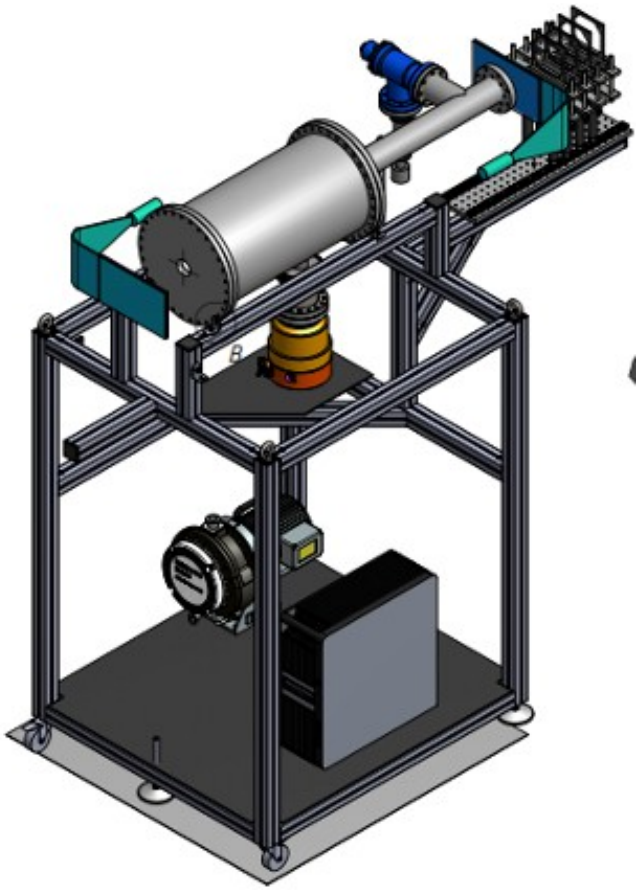

Data analysis: Energy spectra

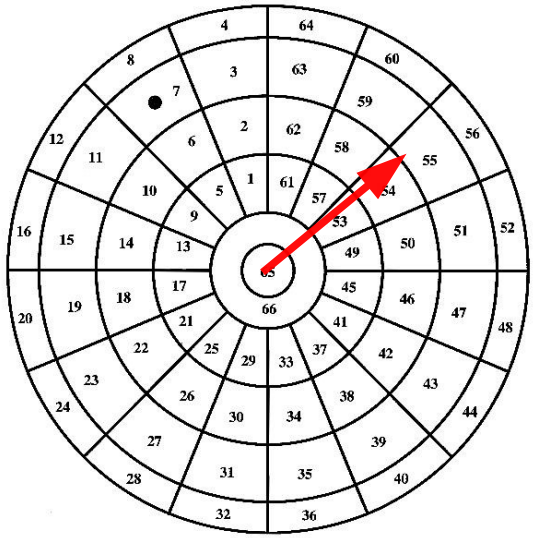

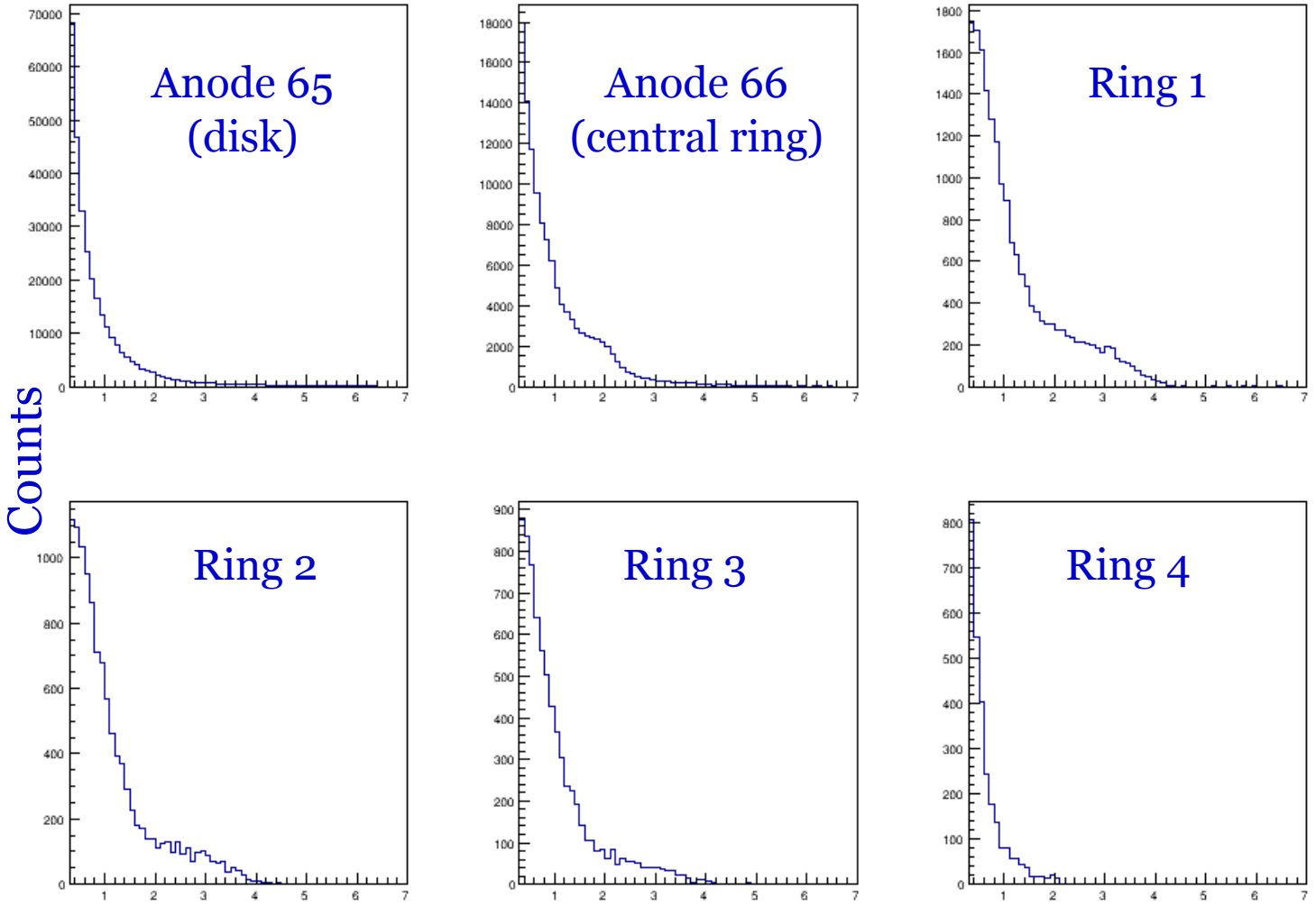

Energy calibration → α-source on the cathode (in front of anode 7)

Data analysis: Identification of recoil fragments

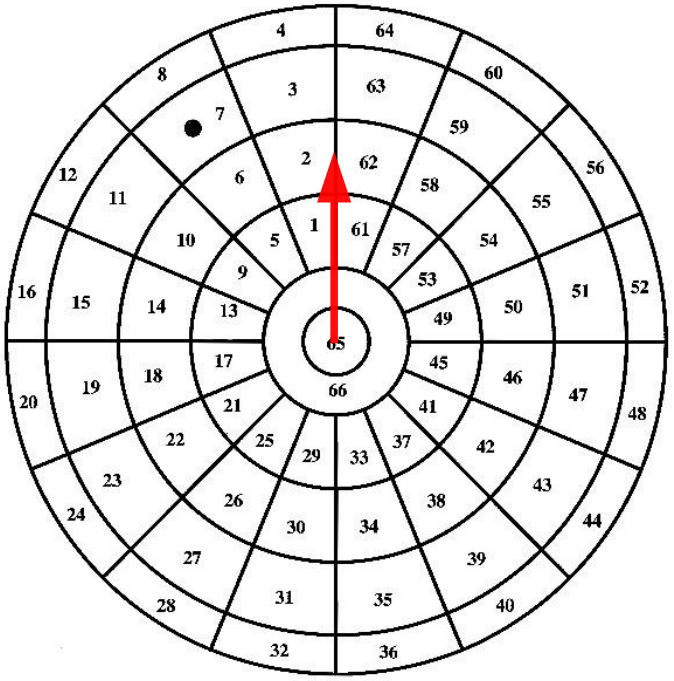

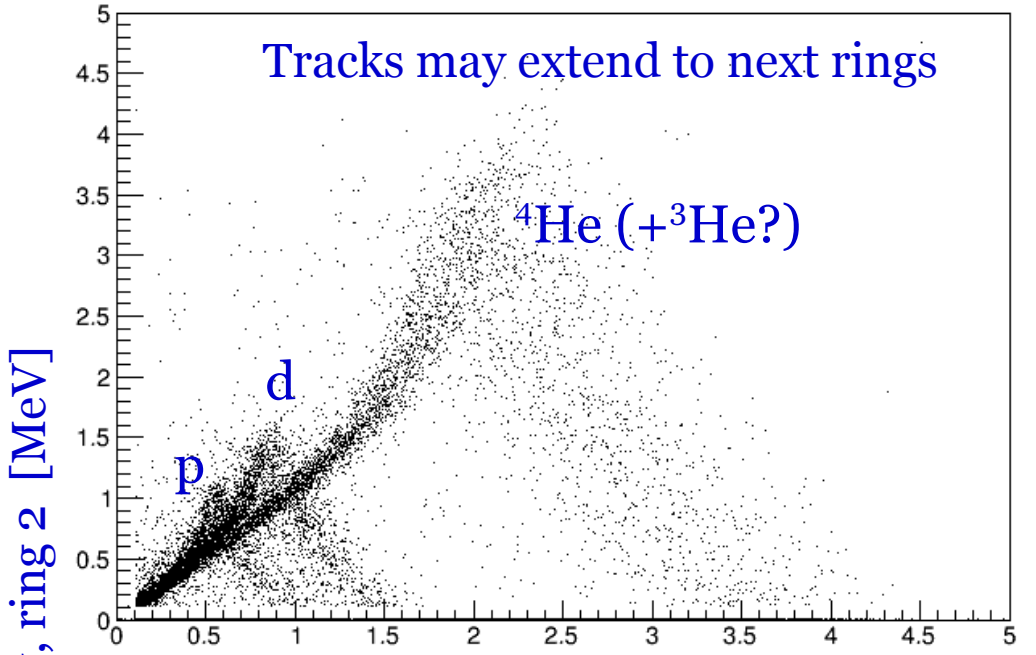

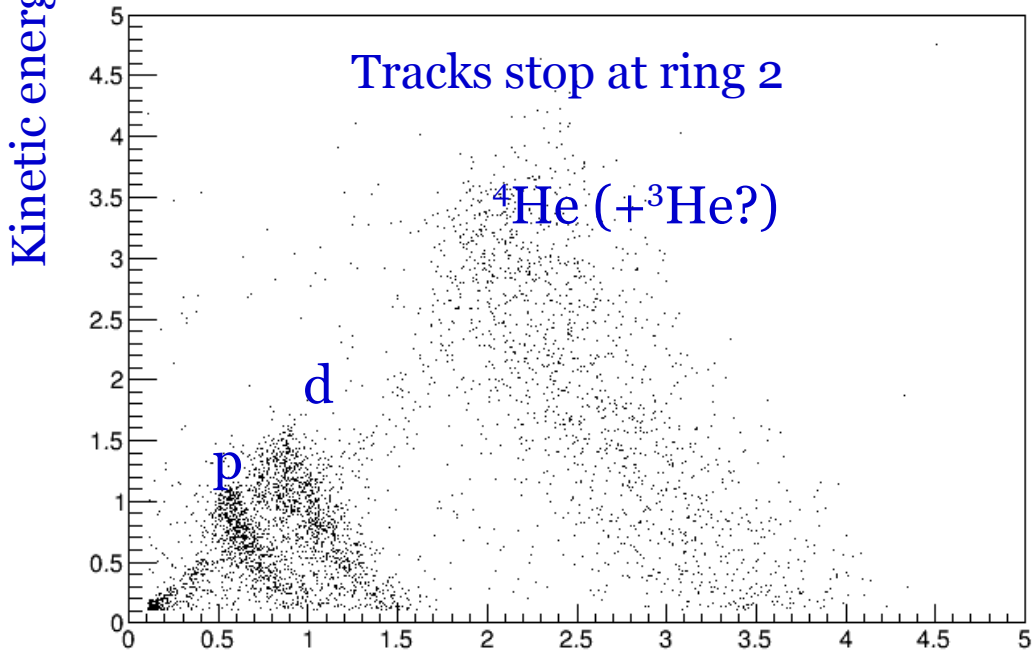

Data analysis: correlation between total energy and Δt

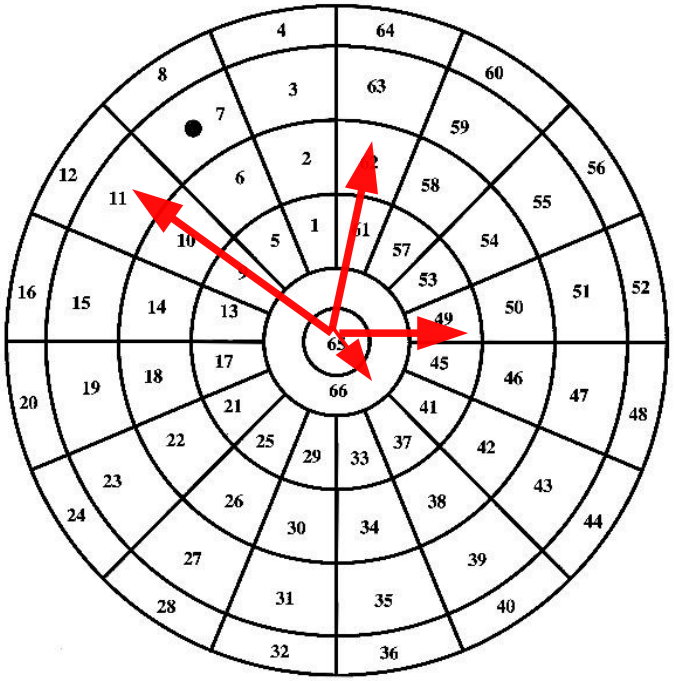

A66 - A65

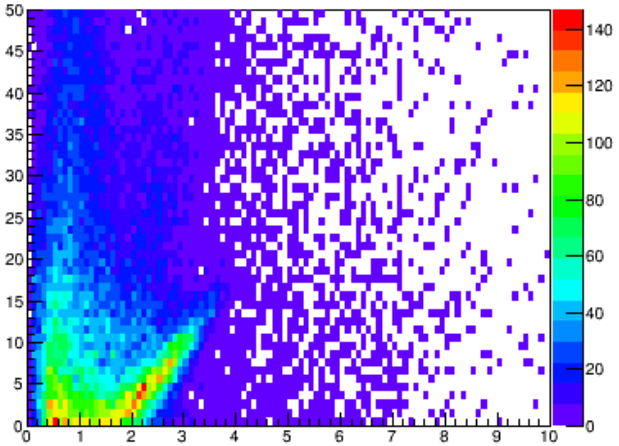

ring1 - A65

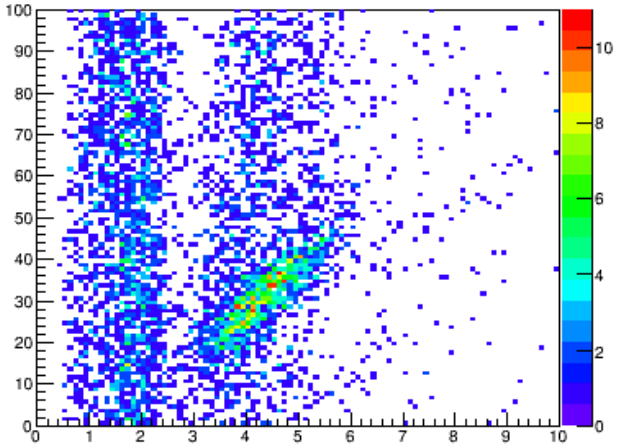

ring2 - A65

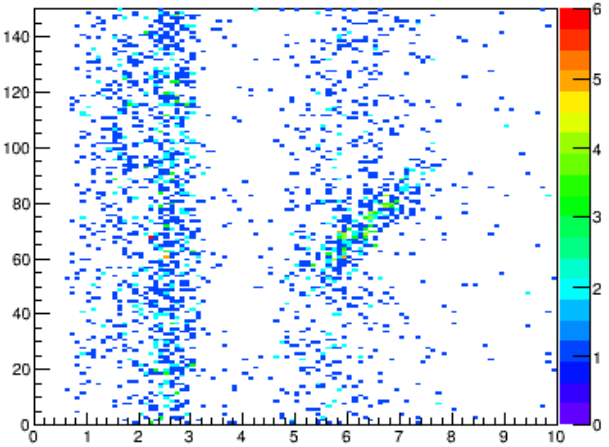

ring3 - A65

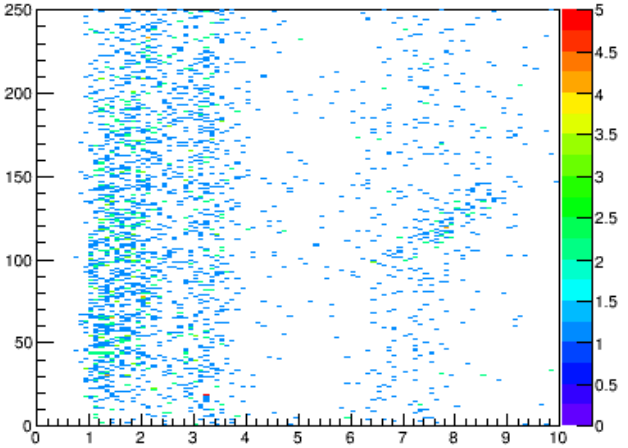

Δt (begin)

Total kinetic energy [MeV]

The tracks had to stop at the "last" ring used in the analysis

→ Access to polar angle and identification of elastic scattering events events

Data analysis: Elastic electron scattering

A66 - A65

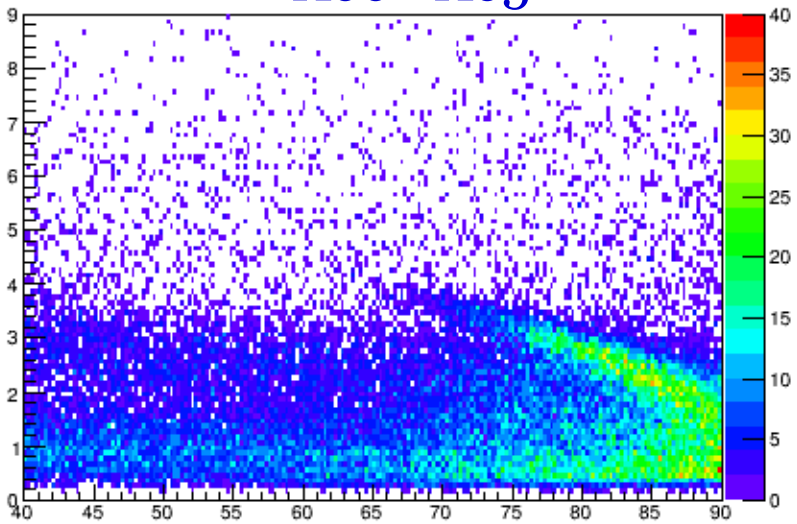

ring1 - A65

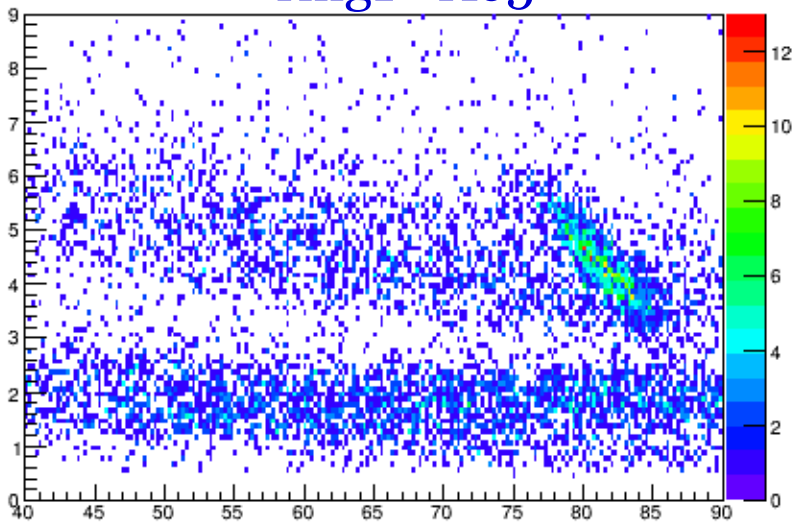

ring2 - A65

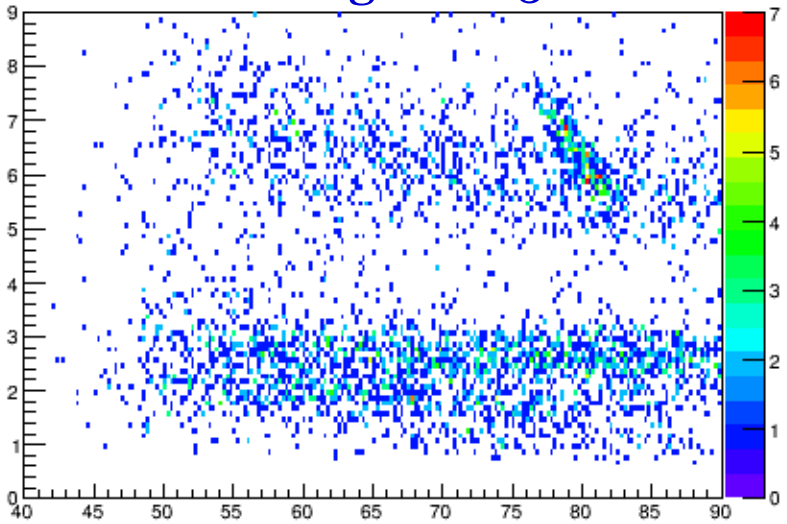

ring3 - A65

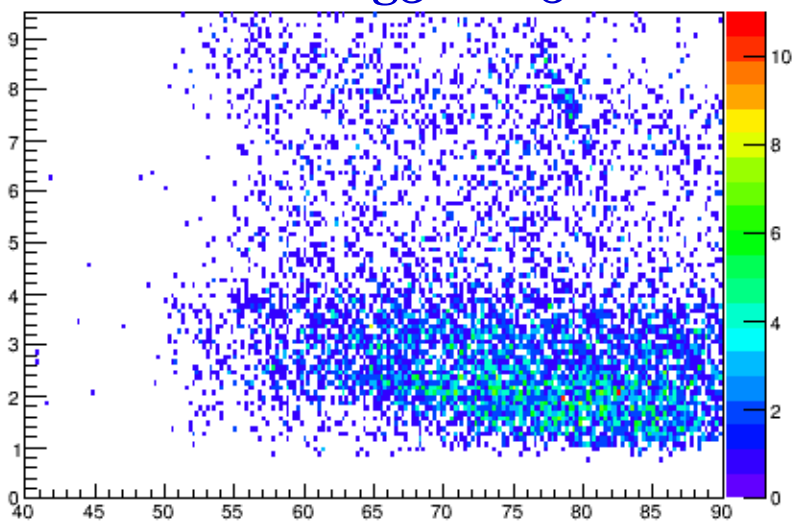

Ekin [MeV]

Theta (recoil) [deg]

Data analysis: Elastic electron scattering

Distortion due to beam instability?

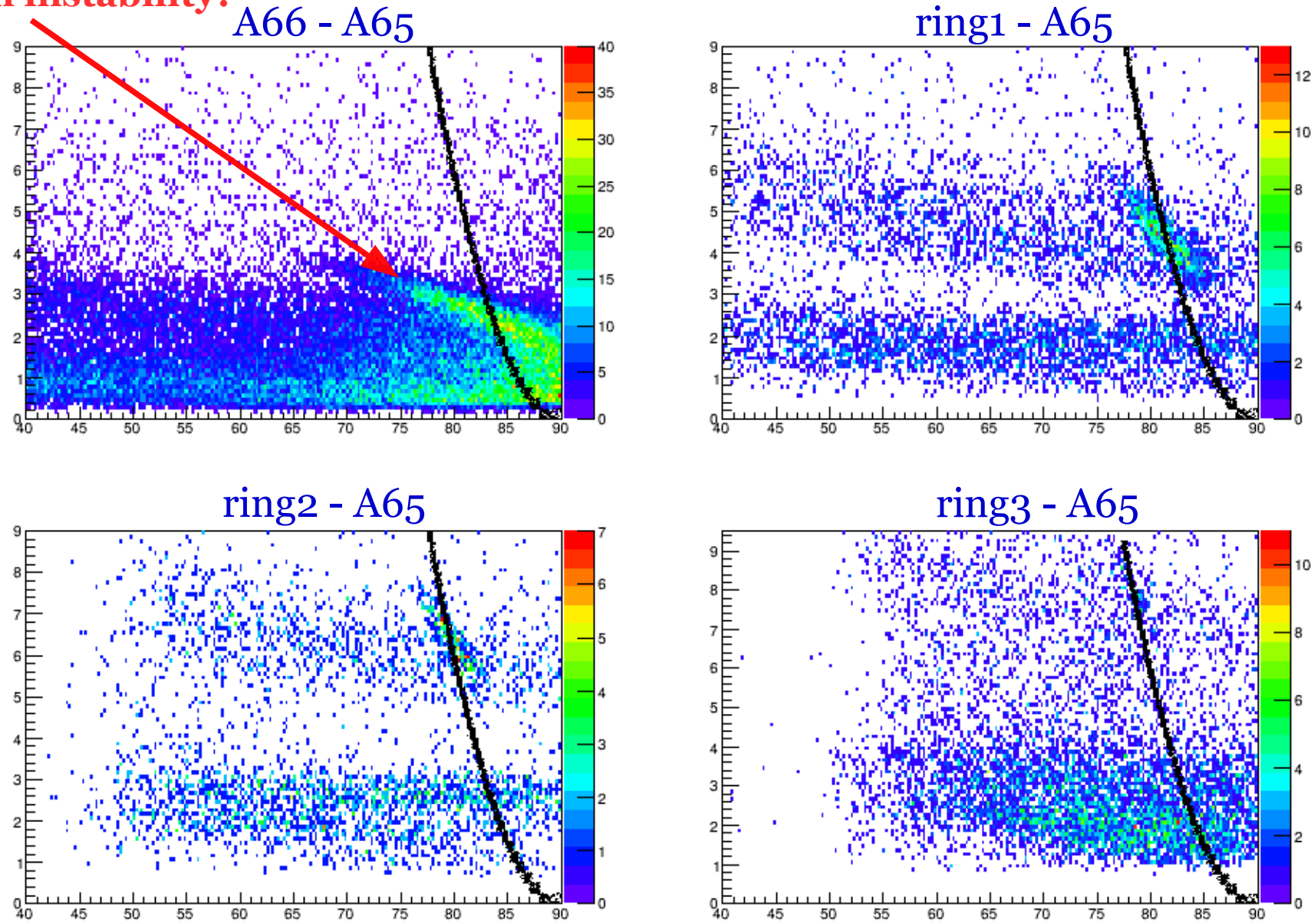

Curve: generated (elastic) ^{4}He events with small energy smearing, (Ebeam = 720 MeV)

Data analysis: Elastic electron scattering

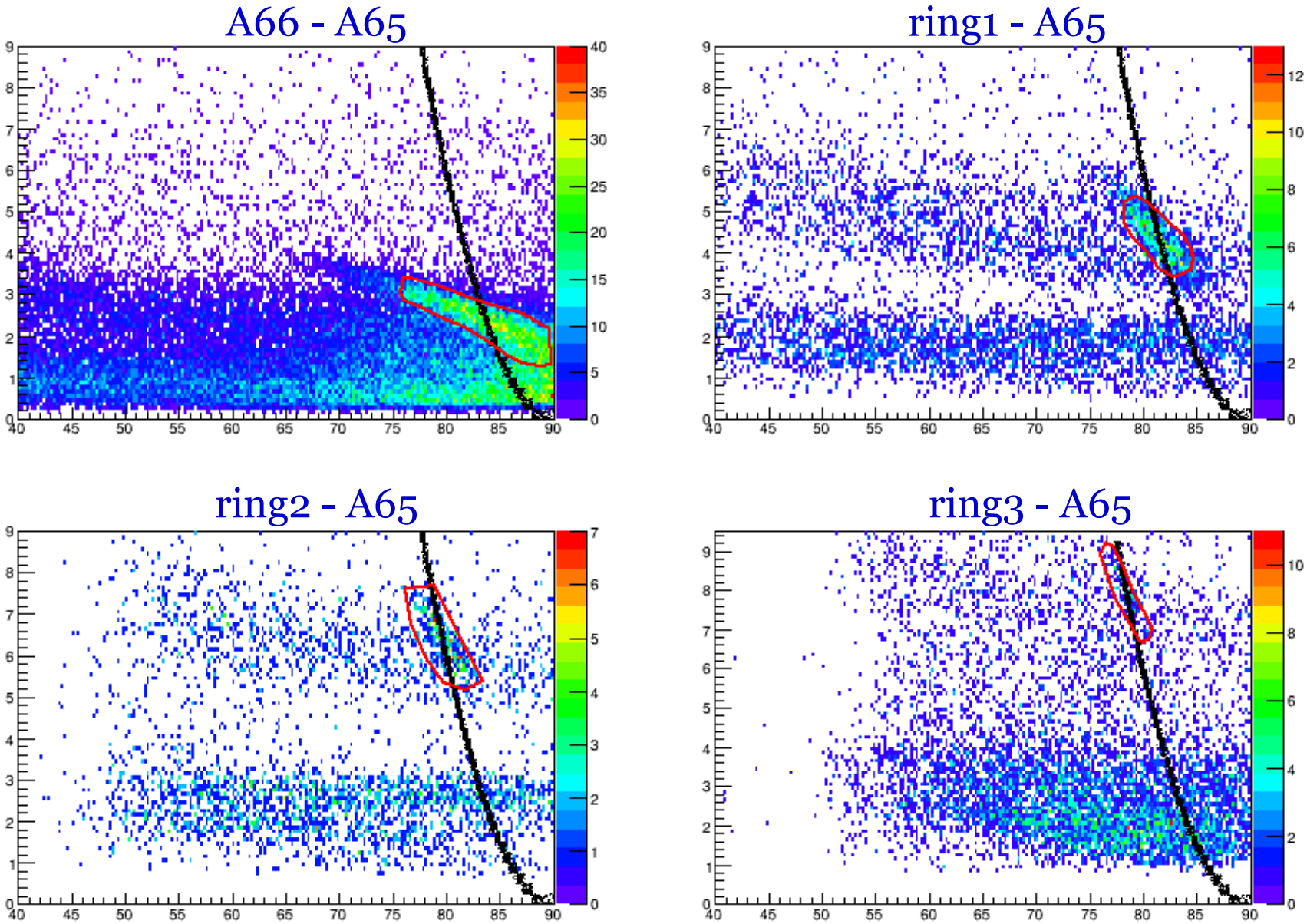

Curve: generated (elastic) ^{4}He events with small energy smearing, (Ebeam = 720 MeV)

Data analysis: Elastic electron scattering

“arbitrary” scaling factor applied

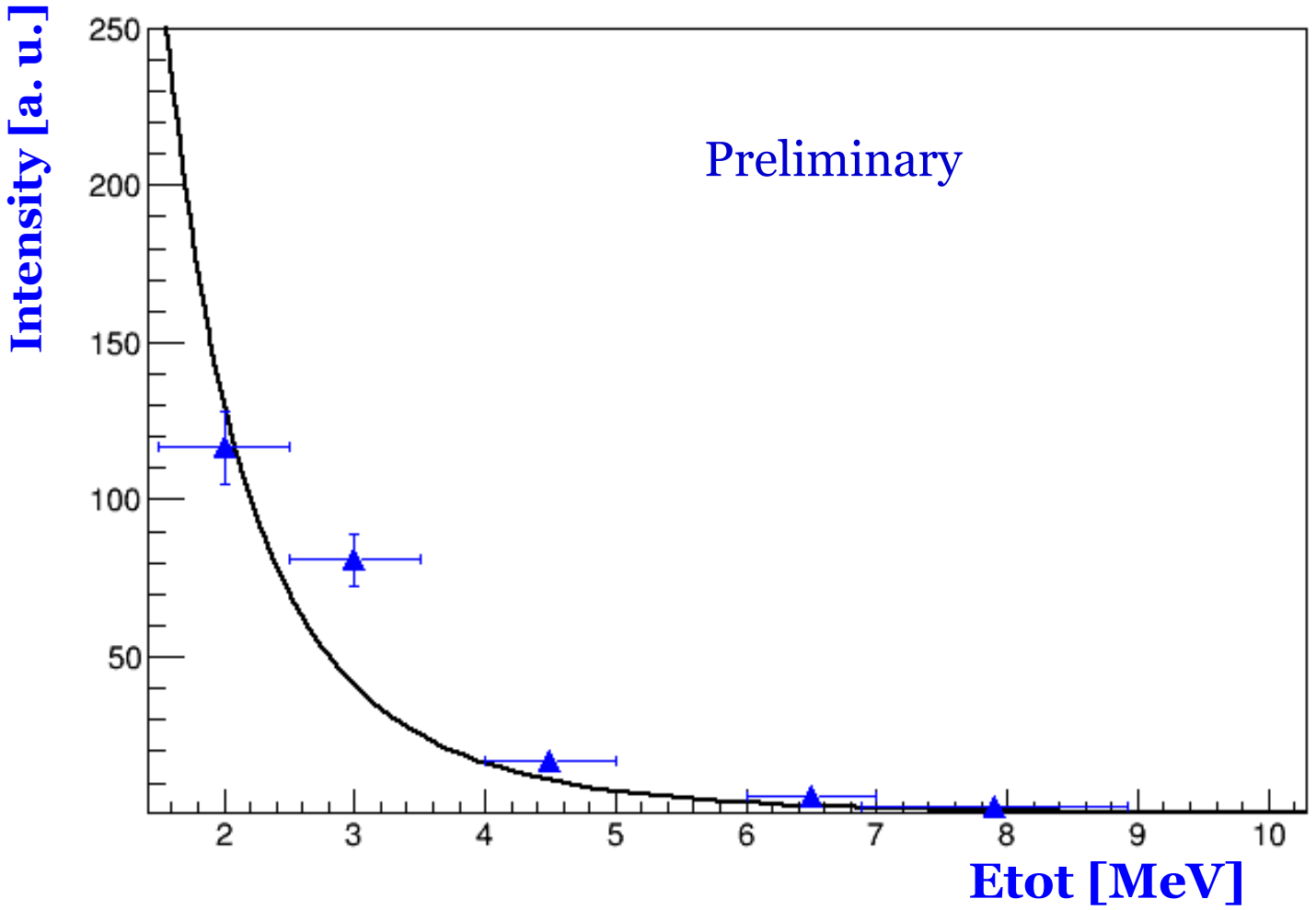

Comparison with ^{4}He elastic scattering cross-section
(for better estimates profile fits are needed)

Suppression of background via correlations

A. Dzyuba (PNPI)

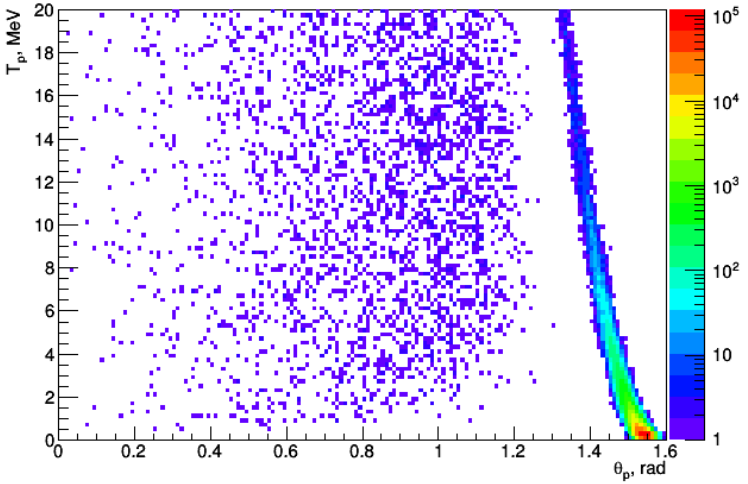

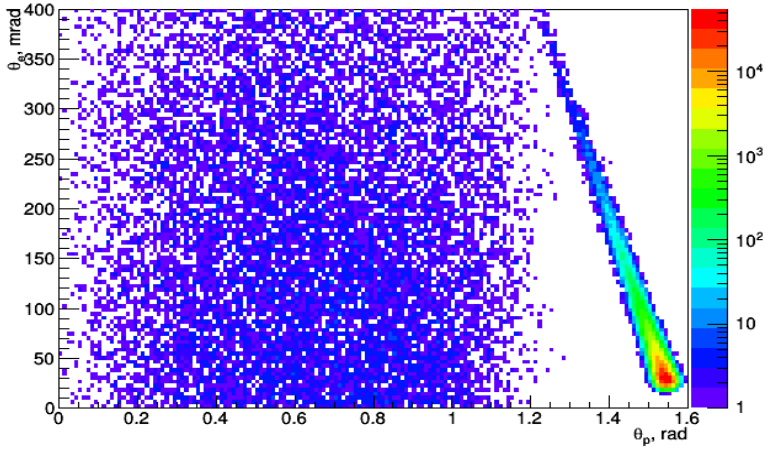

Simulation for the elastic ep scattering and compared with the background reaction $ep \rightarrow ep\pi^0$ for $\varepsilon_e = 720$ MeV

Suppression of background via correlations

A. Dzyuba (PNPI)

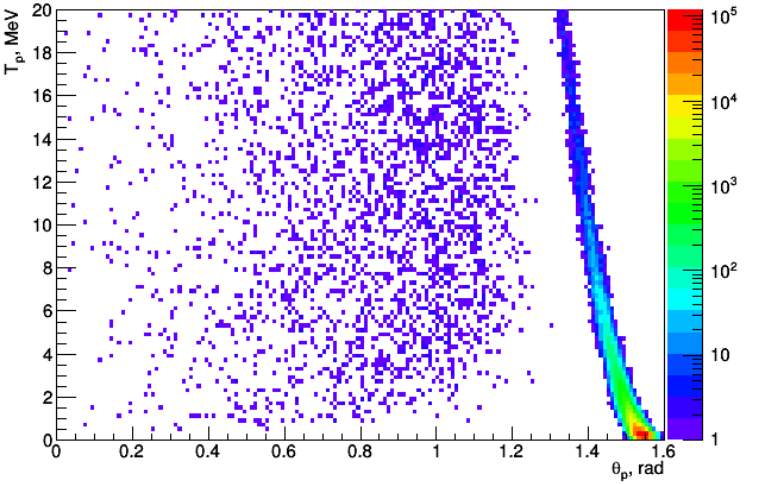

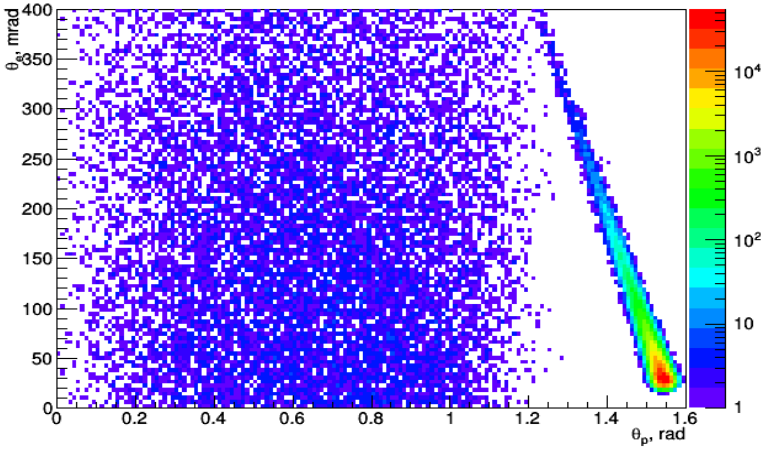

Simulation for the elastic ep scattering and compared with the background reaction $ep \rightarrow ep\pi^0$ for ε_e = 720 MeV

Still possible to distinguish after radiative effects

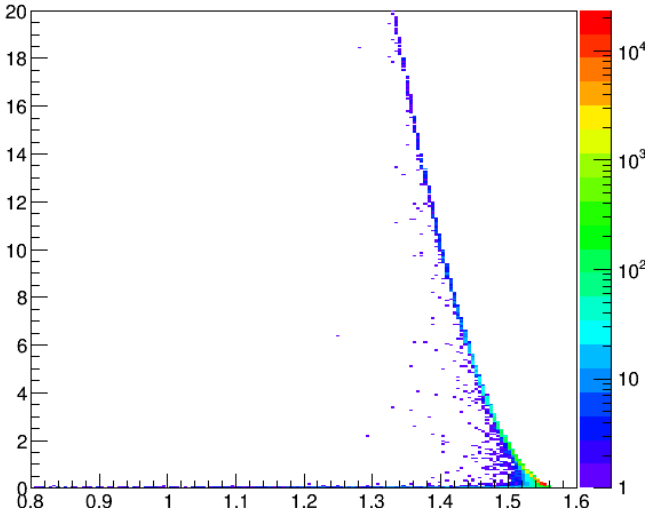

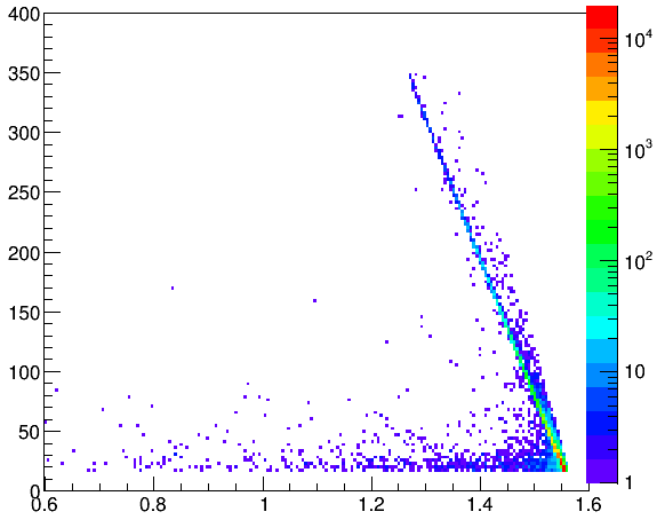

Produced with ESEPP generator taking into account radiative effects
A.V. Gramolin et al., arXiv:1401.2959 (2014)

Suppression of background via correlations

A. Dzyuba (PNPI)

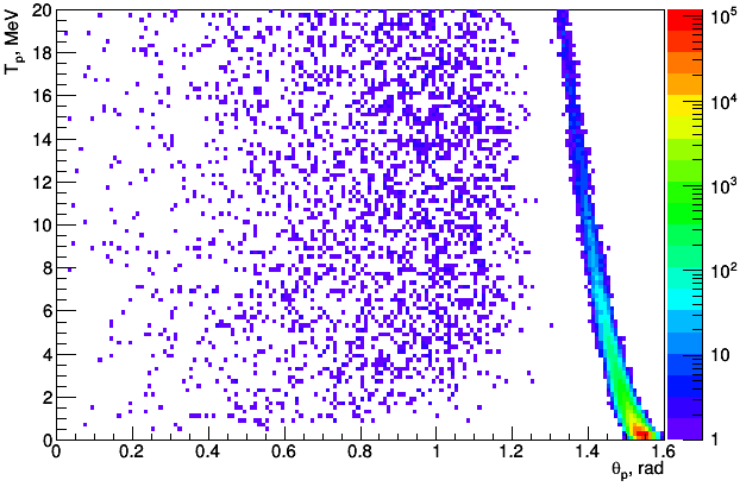

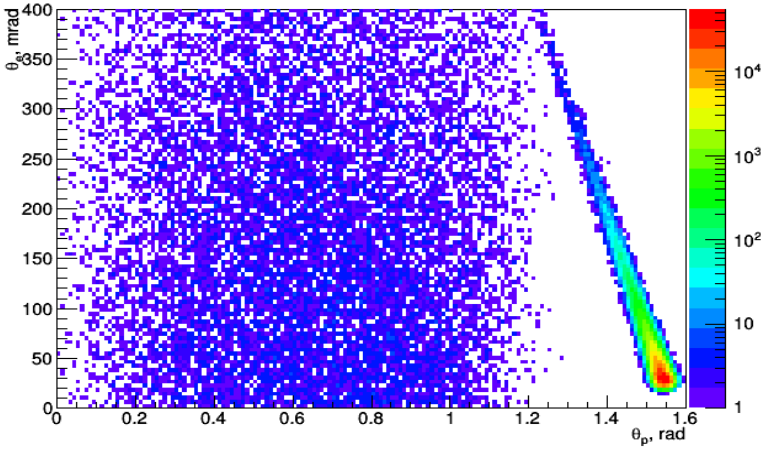

Simulation for the elastic ep scattering and compared with the background reaction ep → epπ⁰ for ε_e = 720 MeV

Still possible to distinguish after radiative effects

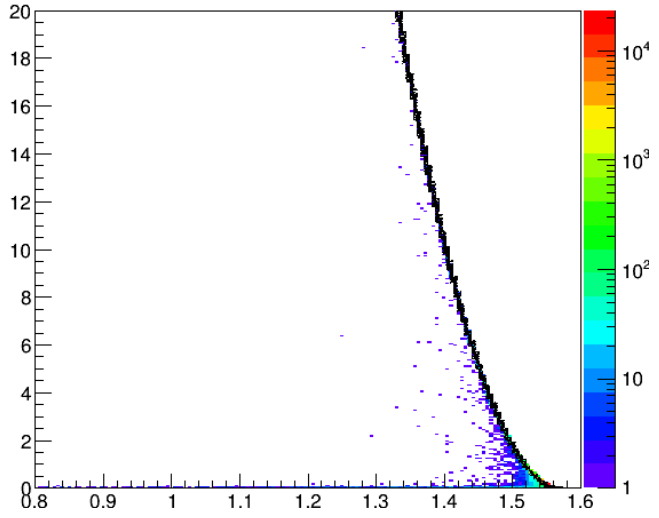

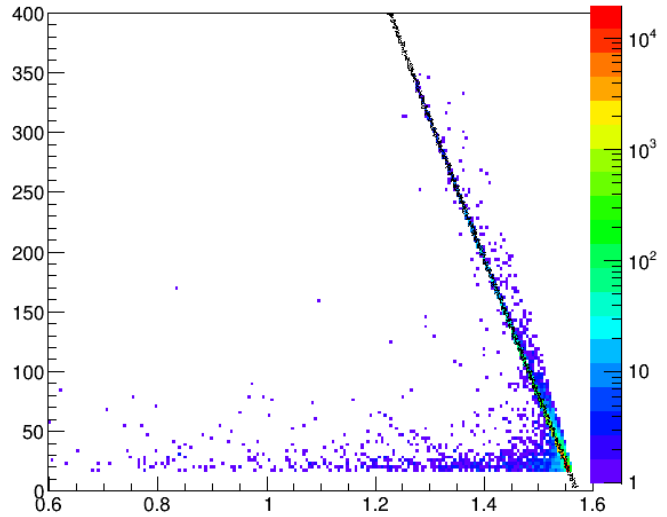

Black area: Phase space with small energy smearing

Produced with ESEPP generator taking into account radiative effects
A.V. Gramolin et al., arXiv:1401.2959 (2014)

Example spectra from the hydrogen run

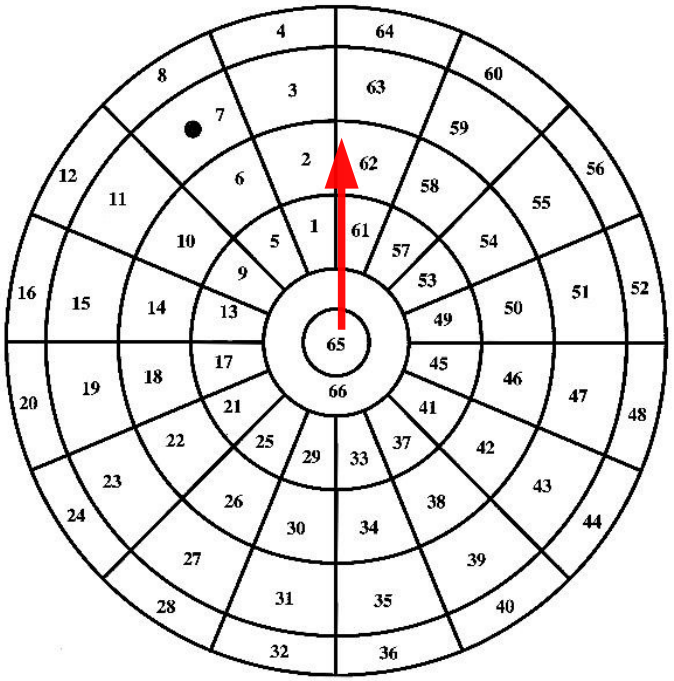

Tracks may extend to next rings

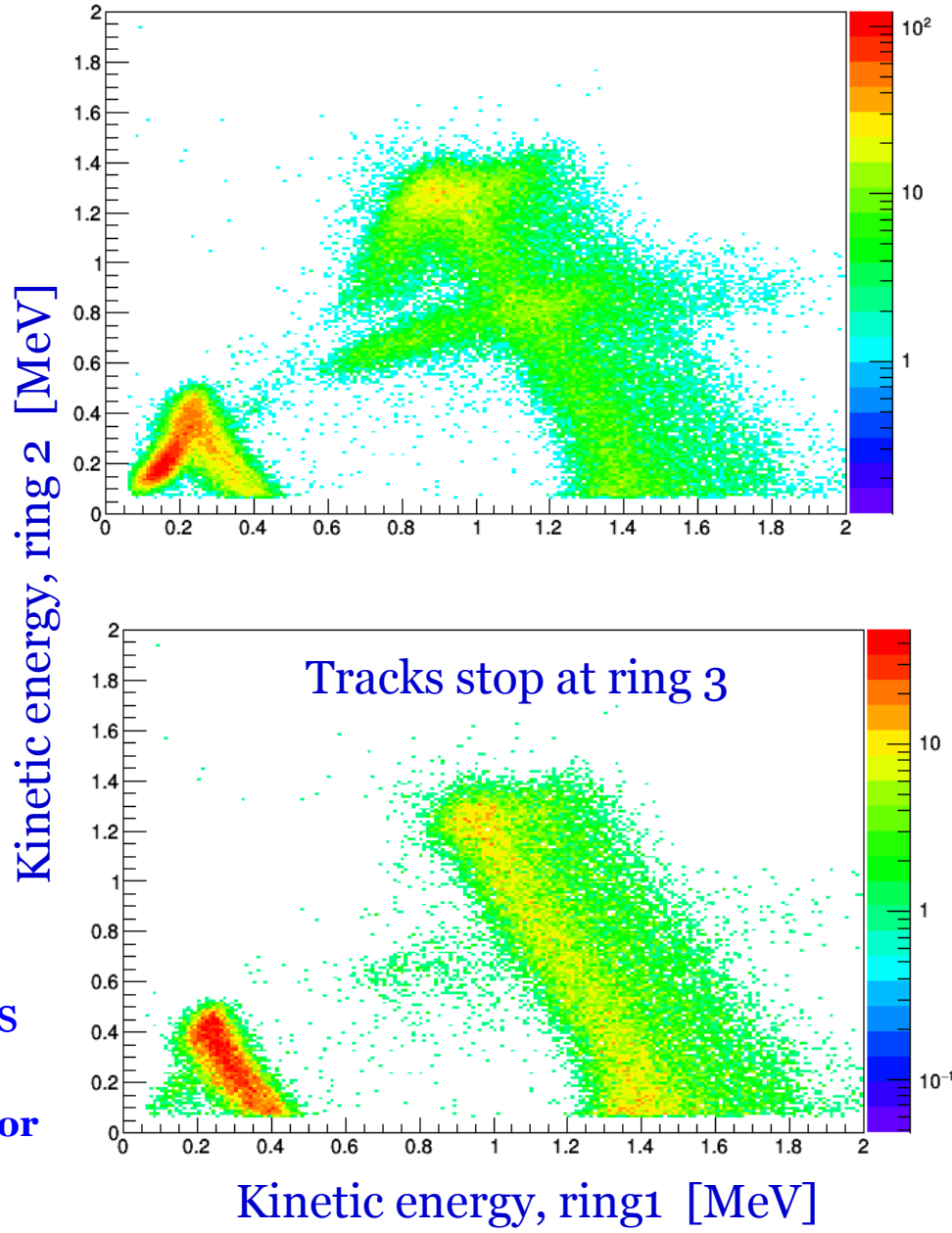

- Previously used algorithms do not work automatically (1.25 bar in the chamber)
- Contamination due to alpha-source
- Correlations are still visible at low energies (ordering)

→ Talk of Evgeny Maev (first cross section estimates for short tracks)

Expected statistical accuracy

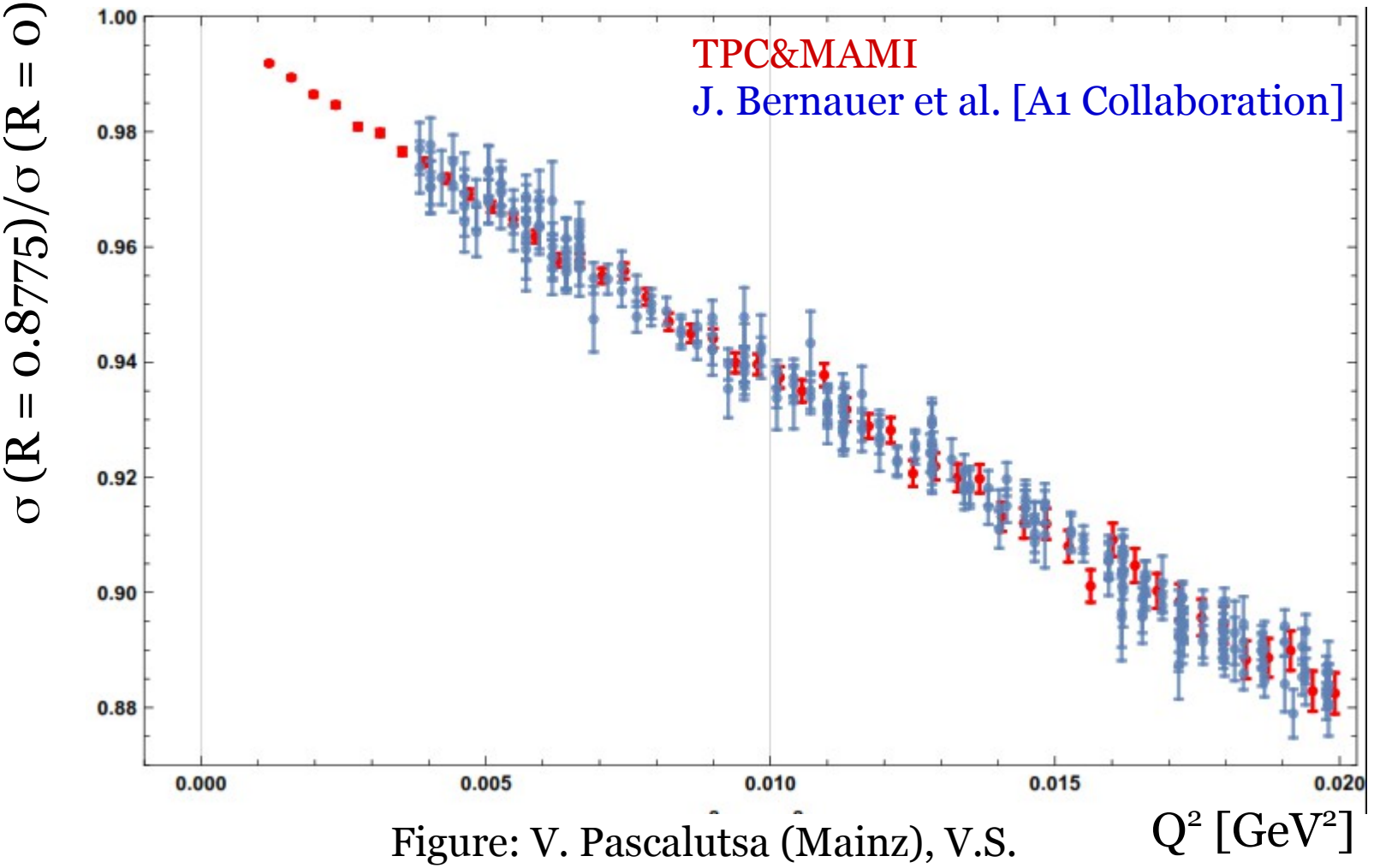

Figure: V. Pascalutsa (Mainz), V.S.

Statistical accuracy for 45 days of data taking (6.8×10^7 events)

Reproduced the analysis from the note prepared at PNPI:

S.Belostotski, N.Sagidova, A.Vorobyev, arXiv:1903.04975 [hep-ph]

Contribution of radiative corrections to the accuracy

Cancellation of the main radiative corrections:

V. S. Fadin, R.E. Gerasimov, Phys. Lett. B 795, 172–176 (2019)

Remaining corrections:

1. Vacuum polarization (1-1.6%), can be calculated with very high accuracy
2. Two-photon exchange can be calculated with ~20% accuracy

(B. Pasquini, and M. Vanderhaeghen Phys. Rev. D 95, 096001 (2017))

→ ~0.05% influence at $Q^2 = 0.02$ GeV^2 and ~0.01% at low Q^2

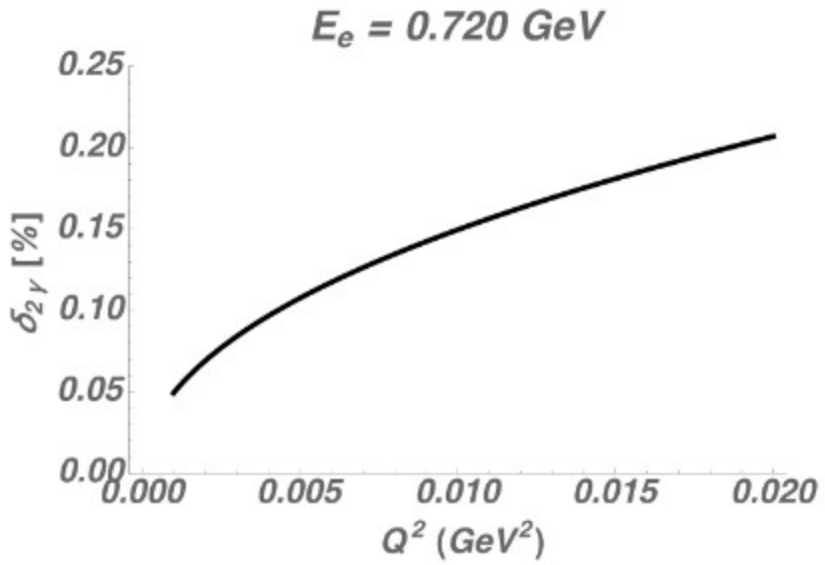

Marc Vanderhaeghen (private communication)

Remaining corrections are smaller compared to the projected experimental accuracy for the cross section (0.2% absolute, 0.1% relative)!

Summary and outlook

Conclusions:

- Analyzed ^{4}He and hydrogen data with software derived from IKAR experiments (at GSI)
- Elastic scattering events identified and very preliminary excitation functions obtained
- Beam position control is crucial for the experiment
- Suppression of backgrounds is still efficient after radiative effects if the information concerning recoil proton is used in the analysis (studies with ESEPP generator)
- Contribution of radiative corrections is lower compared to the projected systematic errors for the experiment

Next steps:

- In the experiment: Controlling beam position → feedback system with MAMI → to be prepared and tested → talk of Alexander Vasilyev in the next session
- Monte Carlo simulations (ideally combined with ESEPP or other generators in the future)
- Data analysis framework?
- Goal for the main experiment – at least two parallel analyses (looking for PhD candidates)

Thank you for your attention!

Many thanks to: Alexey Dzyuba, Alexander Inglessi,
Oleg Kiselev, and Evgeny Maev for your insight on analysis
and
Vladimir Pascalutsa and Marc Vanderhaeghen for theoretical support

Backup

Data analysis: Elastic electron scattering

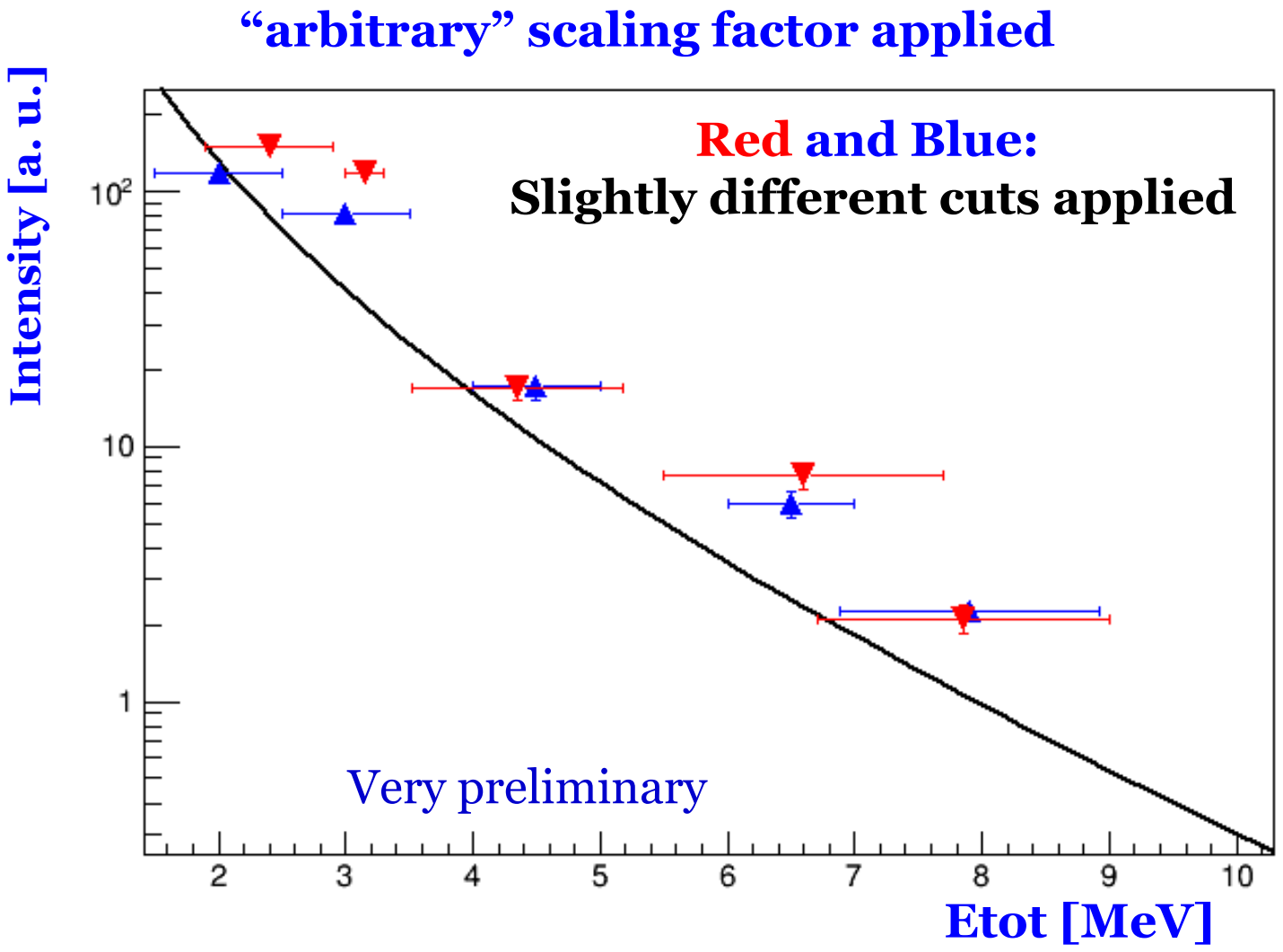

Data analysis: Elastic electron scattering

“arbitrary” scaling factor applied

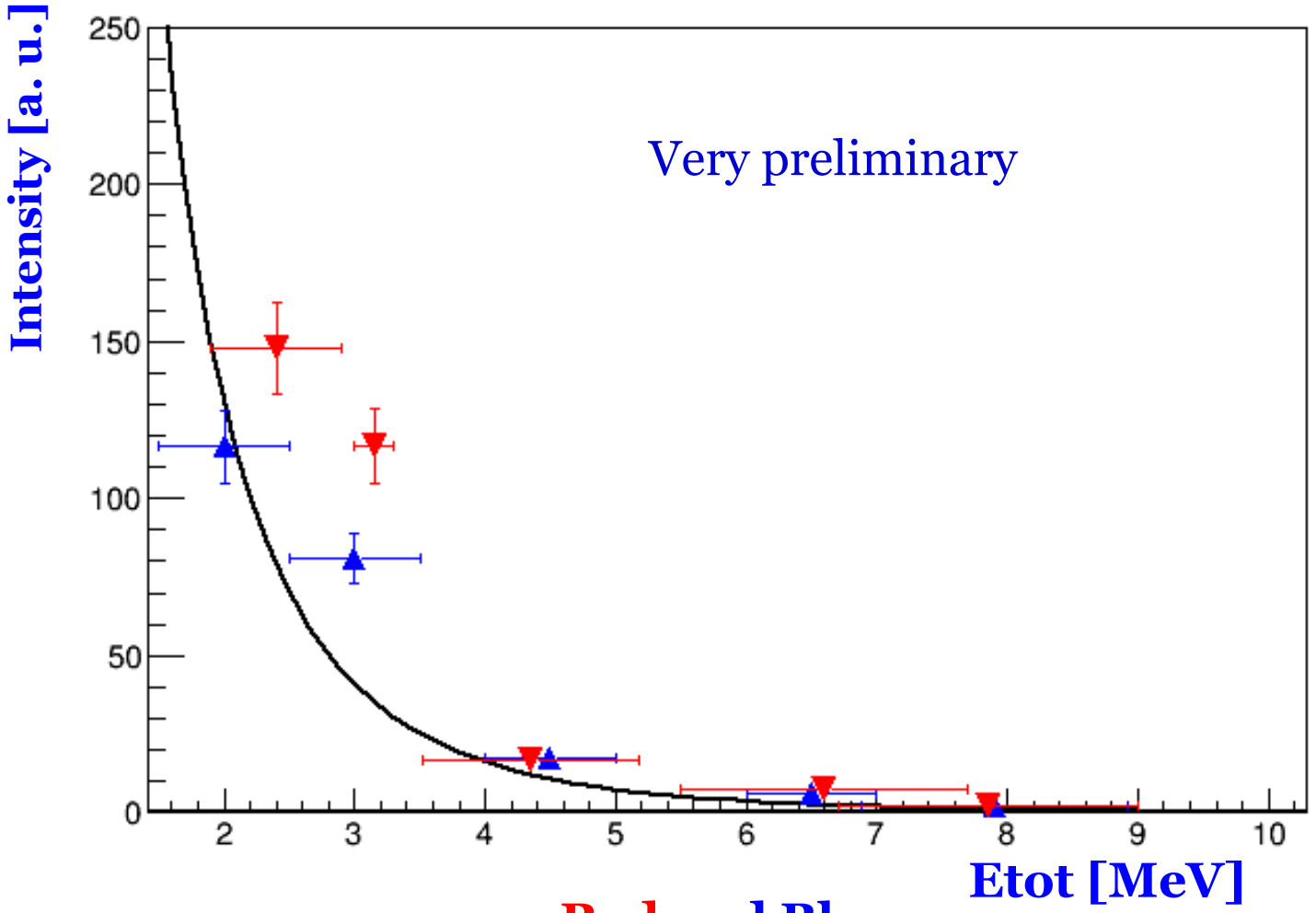

Red and Blue:

Slightly different cuts applied

Main conclusions from the test run

- MAMI electron beam has excellent quality for this experiment
- The beam ionization noise in the central pad is in reasonable agreement with Monte Carlo simulation

Self triggering mode:
Any signal in the anode exceeding 300 keV
Rates:

- ~4 Hz including ~ 1Hz from elastic *e*He scattering at 10 bar with 1.6 MHz beam
- Very low background in the TPC except the central pad
- The low background allows to use TPC in the self-triggering mode

(Alexey Dzyuba, Evgeny Maev, Alexey Vorobyov, ..., PNPI)

Data analysis: Elastic electron scattering

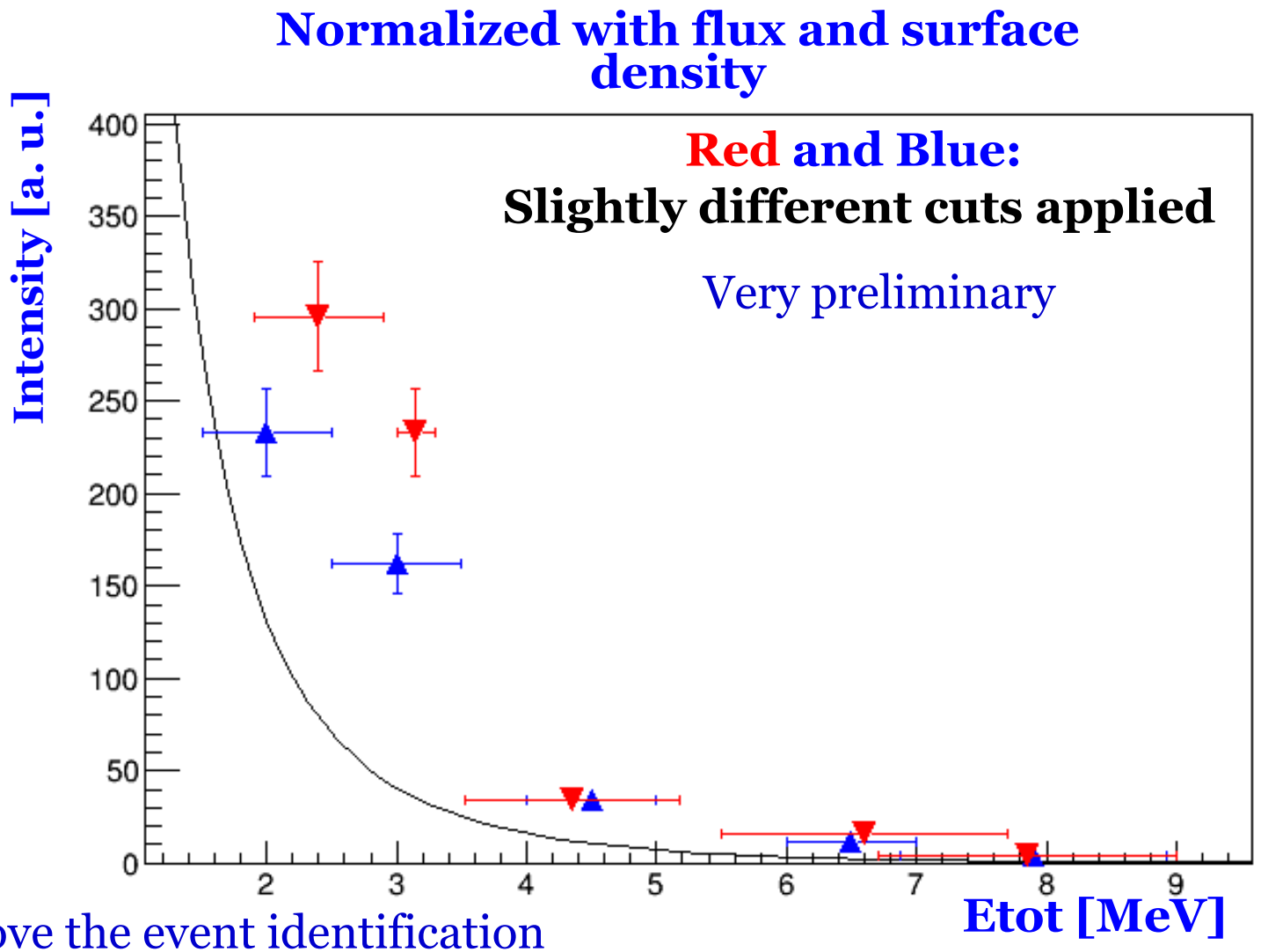

- Improve the event identification
- Control/estimate the background
- Control the beam position (pixel detectors)
- Publish as a proof of principle with upcoming hydrogen (test) data?

Noise from the electron beam (predictions)

Beam ionization noise at the central pad

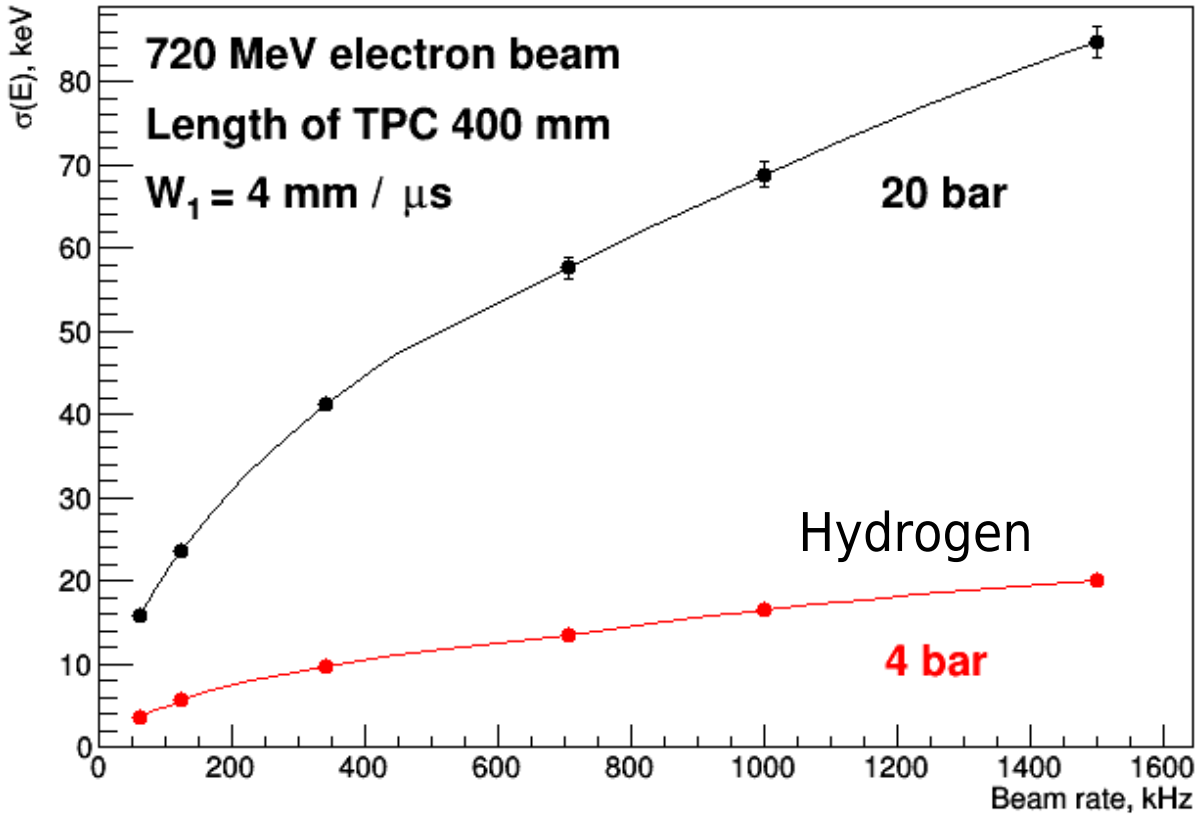

Expected TPC energy resolution in the main experiment at 2 MHz beam rate

90 keV at the central pad, 20-30 keV at the other pads at 20 bar
30 keV at the central pad, 20-30 keV at the other pads at 4 bar

(Alexey Dzyuba, Alexey Vorobyov, PNPI)

Noise from the electron beam

Beam ionization noise at the central pad

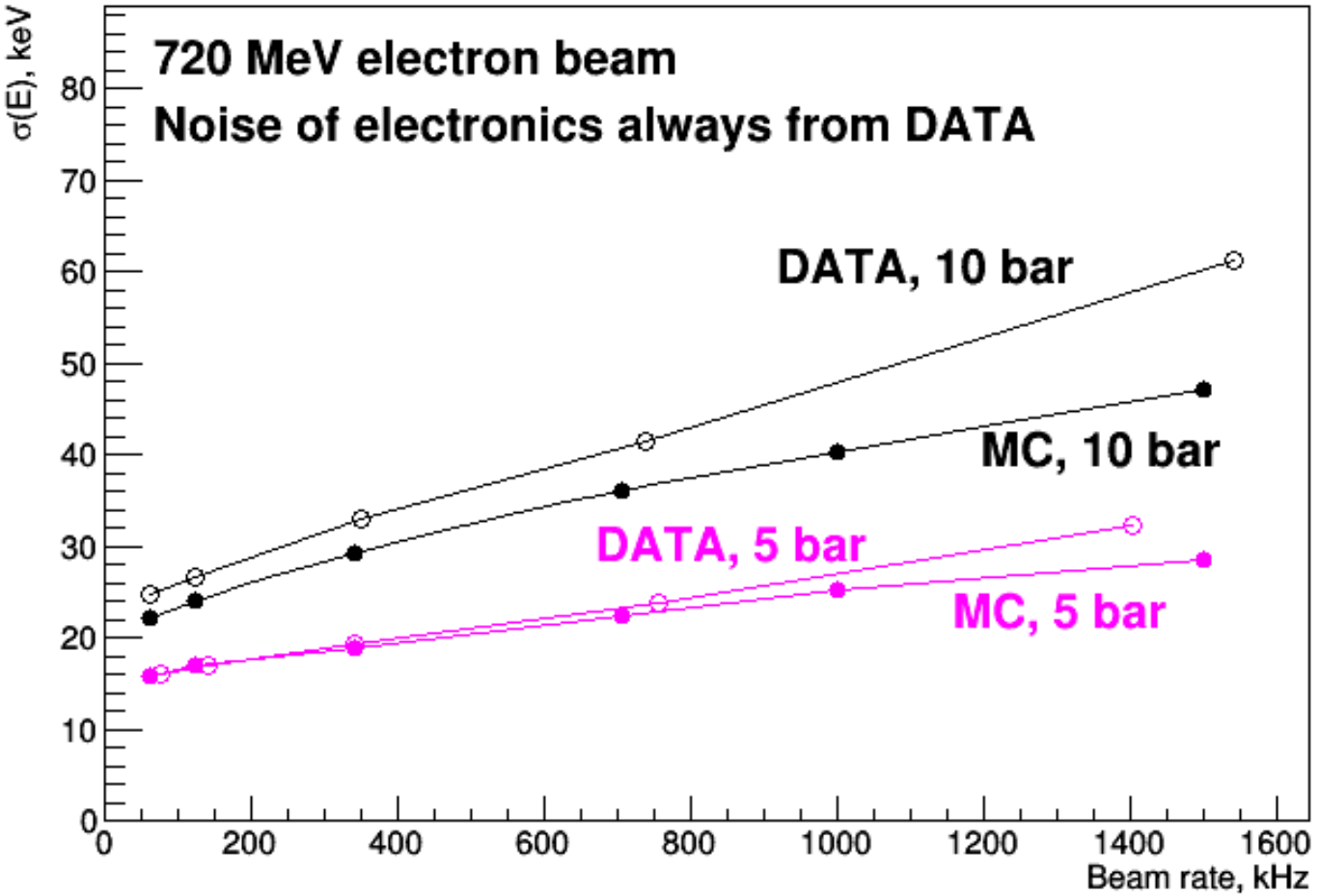

- The beam noise is nearly proportional to the gas pressure
- Measurements are in reasonable agreement with MC
- The beam noise in hydrogen is expected to be smaller than that in the He+4%N_2 mixture by ~ 20%

(Alexey Dzyuba, Alexey Vorobyov, PNPI)

Mainz Microtron and the A2 Hall

Mainz Microtron (MAMI)

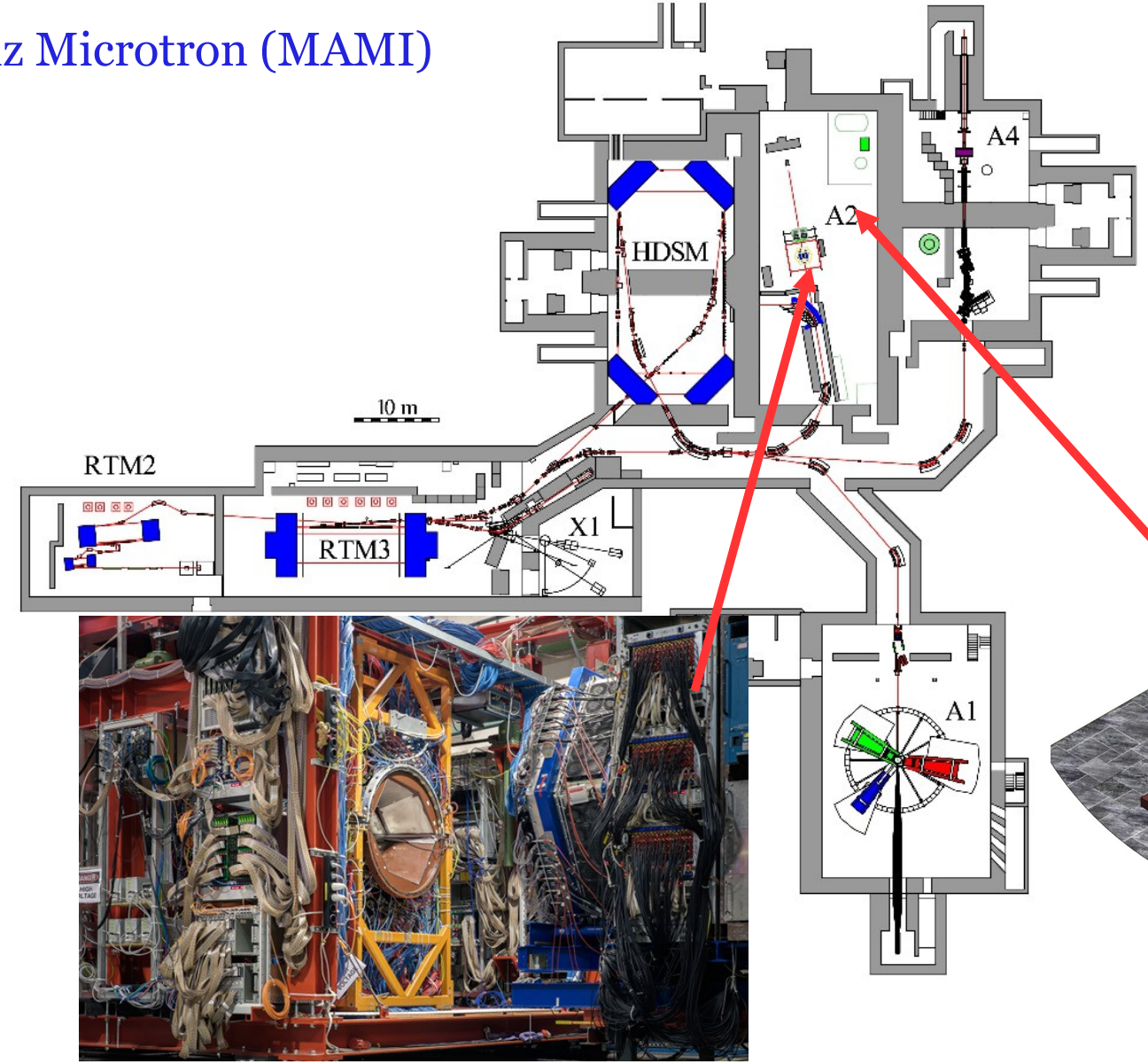

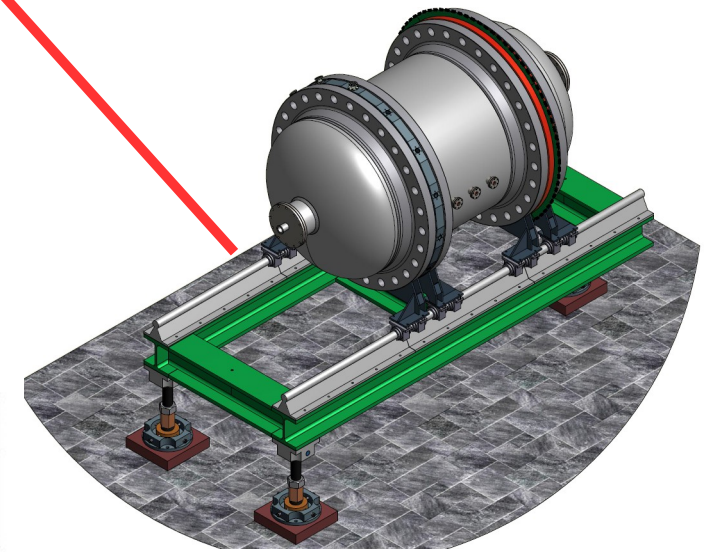

- High-Flux, Tagged, Bremsstrahlung Photon Beam: Unpolarized, Linear, and Circular
- Polarized and Unpolarized Targets
- Electron scattering experiments with a hydrogen TPC (at 720 MeV)

Determination of proton radius

The estimates for the proton radius uncertainties were studied within different analysis frameworks. Within the analysis performed by the group from College of William and Mary [9, 10], the radius was determined by considering the statistical errors only, and in the second version including the total uncertainty (combined statistical and uncorrelated systematic uncertainties). The resulting uncertainty is 0.005 fm if the statistics only and 0.0065 fm for the combination of statistical and uncorrelated systematic errors for the cross section are used in the analysis. A similar analysis was performed by the PNPI group, with a practically model-independent extraction of the proton radius, including high-order terms in the fit. The analysis lead to an uncertainty in order of 0.0085 fm and 0.0045 when some assumptions about the high-order terms are made. The estimates provided above show the order of the expected uncertainty. Indeed, the accuracy may vary dependent on the choice of the fitting function

PRad results

Article

Nature | Vol 575 | 7 November 2019 | 149

A small proton charge radius from an electron–proton scattering experiment

https://doi.org/10.1038/s41586-019-1721-2

Received: 17 June 2019

Accepted: 19 September 2019

Published online: 6 November 2019

W. Xiong[1], A. Gasparian[2]*, H. Gao[1], D. Dutta[3]*, M. Khandaker[4], N. Liyanage[5], E. Pasyuk[6], C. Peng[1], X. Bai[5], L. Ye[3], K. Gnanvo[5], C. Gu[1], M. Levillain[2], X. Yan[1], D. W. Higinbotham[6], M. Meziane[1], Z. Ye[1,7], K. Adhikari[3], B. Aljawrneh[2], H. Bhatt[3], D. Bhetuwal[3], J. Brock[6], V. Burkert[6], C. Carlin[6], A. Deur[6], D. Di[5], J. Dunne[3], P. Ekanayaka[3], L. El-Fassi[3], B. Emmich[3], L. Gan[8], O. Glamazdin[9], M. L. Kabir[3], A. Karki[3], C. Keith[6], S. Kowalski[10], V. Lagerquist[11], I. Larin[12,13], T. Liu[1], A. Liyanage[14], J. Maxwell[6], D. Meekins[6], S. J. Nazeer[14], V. Nelyubin[5], H. Nguyen[5], R. Pedroni[2], C. Perdrisat[15], J. Pierce[6], V. Punjabi[16], M. Shabestari[3], A. Shahinyan[17], R. Silwal[10], S. Stepanyan[6], A. Subedi[3], V. V. Tarasov[12], N. Ton[5], Y. Zhang[1] & Z. W. Zhao[1]

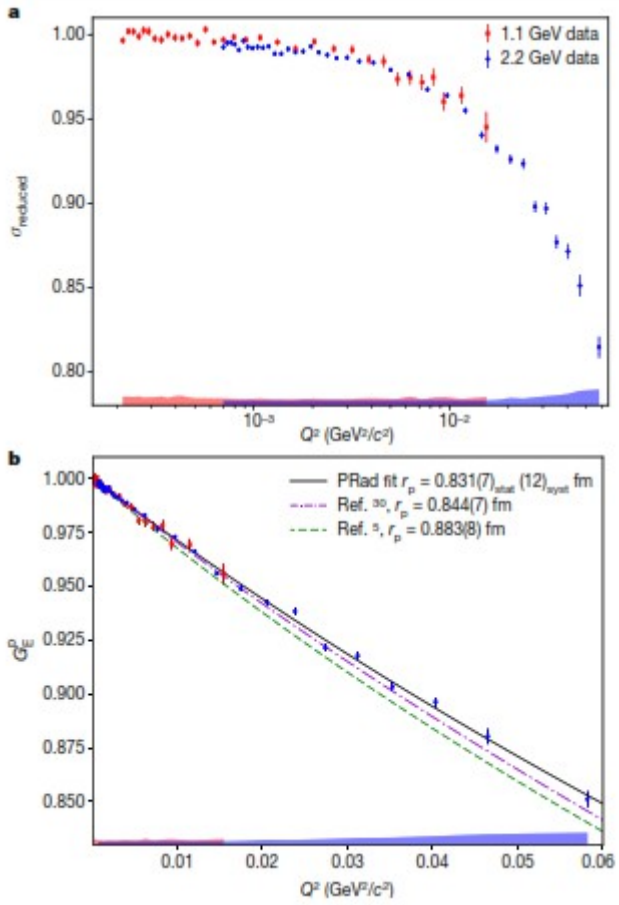

Article

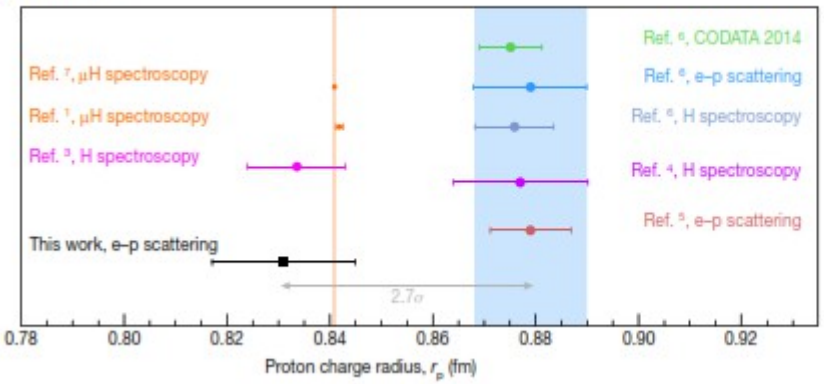

Fig. 4 | The proton charge radius. r_p as extracted from the PRad data in this work, shown alongside other measurements of r_p since 2010 and previous CODATA recommended values. Our result is 2.7σ smaller than the CODATA recommended value for e–p experiments[6]. The orange and blue vertical bands show the uncertainty bounds of the μH and CODATA values for e–p scattering, respectively.

$$r_p = 0.831 \pm 0.007_{stat} \pm 0.012_{syst}\ \text{fm}$$

PNPI note

Proton radius reconstruction from simulated electron-proton elastic scattering cross sections at low transfer momenta

S.Belostotski, N.Sagidova, A.Vorobyev

Petersburg Nuclear Physics Institute

For this analysis, the ep scattering events were generated according to the following function describing the ep elastic scattering differential cross section:

$$\frac{d\sigma}{dt} = \frac{\pi\alpha^2}{t^2}\left\{G_E^2\left[\frac{(4M+t/\varepsilon_e)^2}{4M^2-t}+\frac{t}{\varepsilon_e^2}\right]-\frac{t}{4M^2}G_M^2\left[\frac{(4M+t/\varepsilon_e)^2}{4M^2-t}-\frac{t}{\varepsilon_e^2}\right]\right\}\text{GeV}^{-4}, \quad (1)$$

where $-t = Q^2$; $\alpha = 1/137.036$; M is the proton mass ($M = 938.272$ MeV); ε_e is the total electron energy (ε_e =720.5 MeV); $G_E(Q^2)$ and $G_M(Q^2)$ are the electric and magnetic form factors, respectively. We have accepted the following approximation valid for the small Q^2 region:

$$G_M(Q^2) = \mu_p \cdot G_E(Q^2) = 2.793 G_E(Q^2). \quad (2)$$

$G_E(Q^2)$ is taken as a power series expansion:

$$G_E(Q^2) = 1 - R2\cdot B_2\cdot Q^2/C_2 + R4\cdot B_4\cdot Q^4/C_4 - R6\cdot B_6\cdot Q^6/C_6 + R8\cdot B_8\cdot Q^8/C_8, \quad (3)$$

where $B_n = (5.06773)^n$, $C_n = (n+1)!$, n=2,4,6,8; $R2 = < r_p^2 >$, $R4 = < r_p^4 >$, $R6 = < r_p^6 >$, and $R8 = < r_p^8 >$. The *rms*-radius $R_p = (R2)^{1/2}$. In such presentation, $< r_p^n >$ and Q^n are expressed in fm^n and in GeV^n, respectively. 1 fm = 5.06773 GeV^{-1}; 1 GeV^{-2} = 0.389379 mb.

The ep scattering events were generated in the Q^2 range from 0.001 GeV^2 to 0.04 GeV^2 using the values of $R2$, $R4$, $R6$, and $R8$ obtained by J.C.Bernauer [5,6] from analysis of the cross sections measured in the A1 experiment:

$$R2 = 0.7700 \text{ fm}^2,\ R4 = 2.63 \text{ fm}^4,\ R6 = 26 \text{ fm}^6,\ R8 = 374 \text{ fm}^8.$$

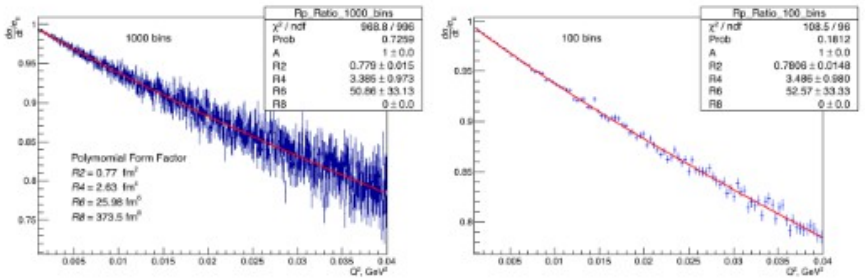

Figure 2: Distribution of the ratio of $d\sigma/dt$ (R_p= 0.8775 fm) / $d\sigma/dt$ (R_p= 0), equivalent to the G_E^2 (Q^2) distribution, obtained according to eq.(6).
Statistics: $N_{ev}(R_p = 0.8775 \text{ fm}) = 6.9636 \cdot 10^7$ events, $N_{ev}(R_p = 0) = 7.\ 13227 \cdot 10^9$ events. Binning: 1000 bins (left panel) and 100 bins (right panel). Red lines show the results of the fit with the form factor represented by Fit 1 in Table 1.

Table 5: Statistical and systematic errors in R_p resulted in the fits of the psuedo-data with a polynomial function $G_E(Q^2) = A\cdot(1 - < r_p^2 > \cdot B_2\cdot Q^2/C_2 + < r_p^4 > \cdot B_4\cdot Q^4/C_4 - < r_p^6 > \cdot B_6\cdot Q^6/C_6 + < r_p^8 > \cdot B_8\cdot Q^8/C_8)$ with three or four free parameters. Statistics : $7\cdot 10^7$ ep scattering events in the Q^2 range 0.001 GeV^2 $\le Q^2 \le$ 0.04 GeV^2.

	Free parameters	Fixed parameters	ΔR_p (stat)	ΔR_p (syst)	comments
Option1	$A < r_p^2 > < r_p^4 > < r_p^6 >$	$< r_p^8 >$	$\pm$ 0.0085 fm	< 0.001fm	—
Option2	$A < r_p^2 > < r_p^4 >$	$< r_p^6 > < r_p^8 >$	$\pm$ 0.0042 fm	$\pm$ 0.0025 fm < 0.001fm	$< r_p^6 >$ from[6] $< r_p^6 >$ from[7]

Systematic errors

1	Drift velocity, W1	0.01%
2	High Voltage, HV	0.01%
3	Temperature, K	0.015 %
4	Pressure, P	0.01%
5	H_2 density , ρ_p	0.025 %
6	Target length, L_{tag}	0.02 %
7	Number of protons in target, N_p	0.045 %
8	Number of beam electrons, N_e	0.05 %
9	Detection efficiency	0.05 %
10	Electron beam energy, ε_e	0.02 %
11	Electron scattering angle, θ_e	0.02 %
12	t-scale calibration, T_R relative	0.04 %
13	t-scale calibration, T_R absolute	0.08 %
	$d\sigma/dt$, relative	0.1%
	$d\sigma/dt$, absolute	0.2%

Test setup and beam monitoring system

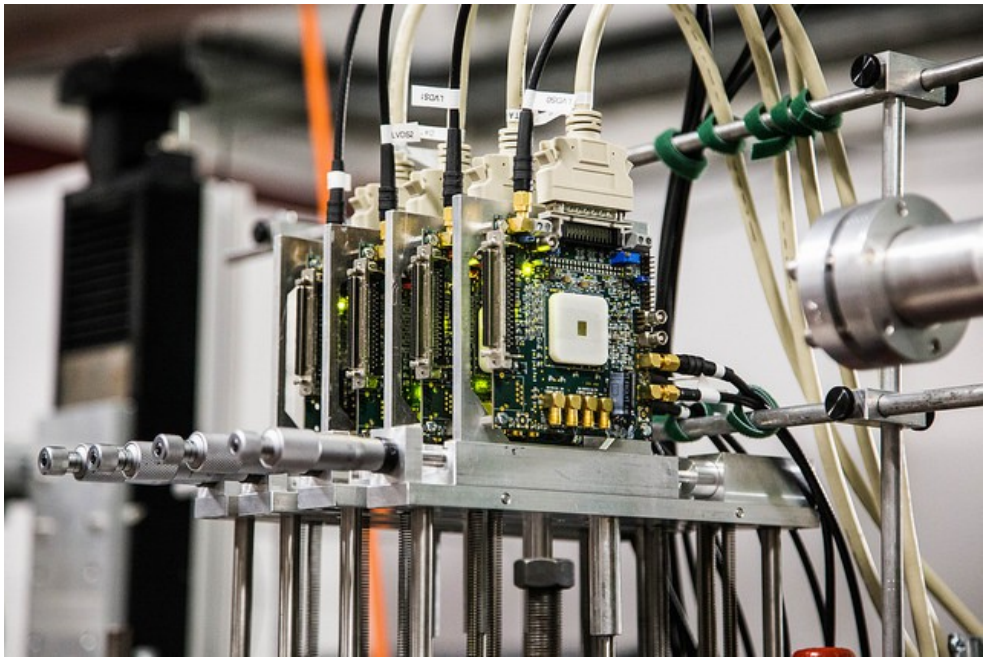

4-layer HV-MAPS pixel detector (3x3 mm)

Monitoring the beam position, reconstruction of electron tracks, and determination of the electron flux

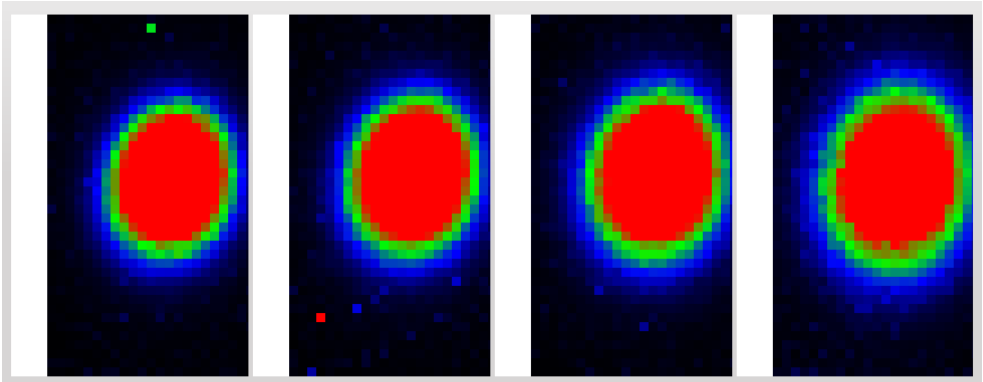

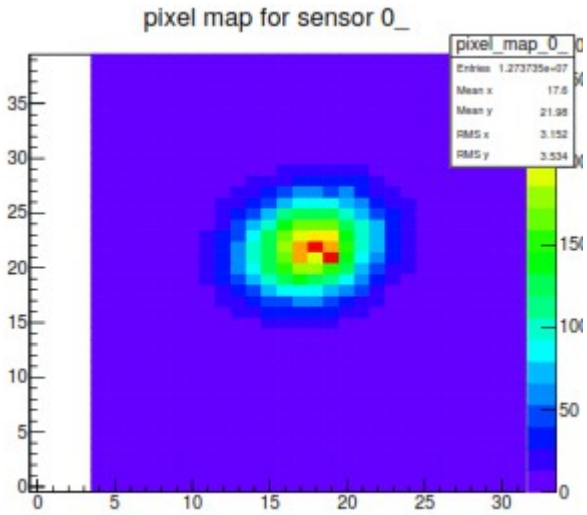

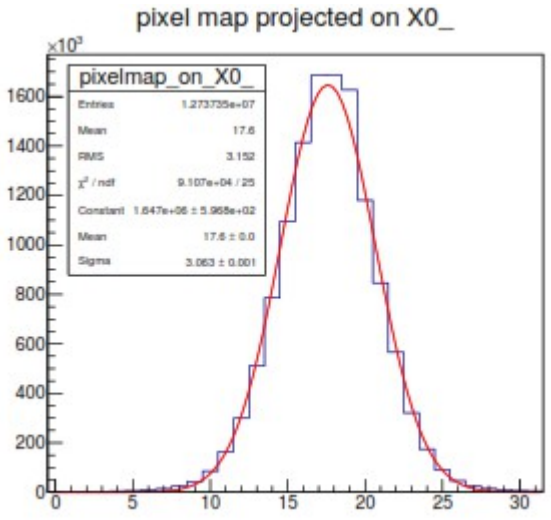

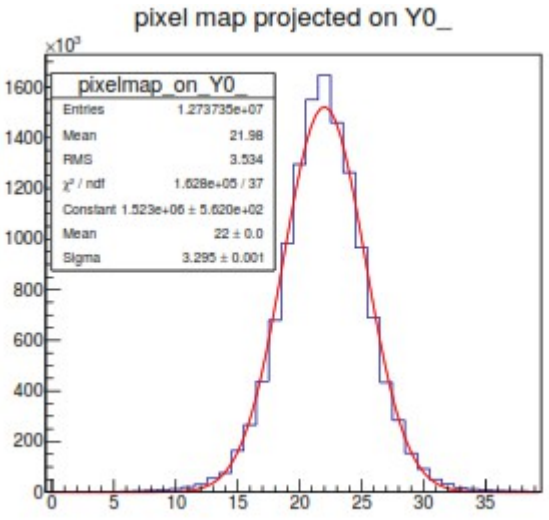

Run conditions and acquired data

- The main run: 10 bar pressure, electron beam intensity ~ 1.4 MHz (counted by the upstream scintillator): ~100 hours, acquired ~2000 files. ~2.5x10^6 events (total)

- Low intensity tests: (130kHz, 90files) and (300kHz, 150 files)

In the end of the experiment: the gas pressure in the TPC was decreased down to 5bar (HV on cathode ~9kV), beam intensity ~ 1.35 MHz, ~35 hours were collected ~ 350 files,~ 4x10^6 events (total)

See the talk of A. Dzyuba for further details and results

Data:

- ~2.1 TB from the TPC and scintillators and 3.7 TB from the pixel telecsope
- Stored at GSI at two different locations and will be copied to the machines in Mainz in the near future
- Analysis and simulation steps to be discussed (Patrik Adlarson, Alexey Dzyuba, Timothy Hayward, Alexander Inglessi, V.S.)

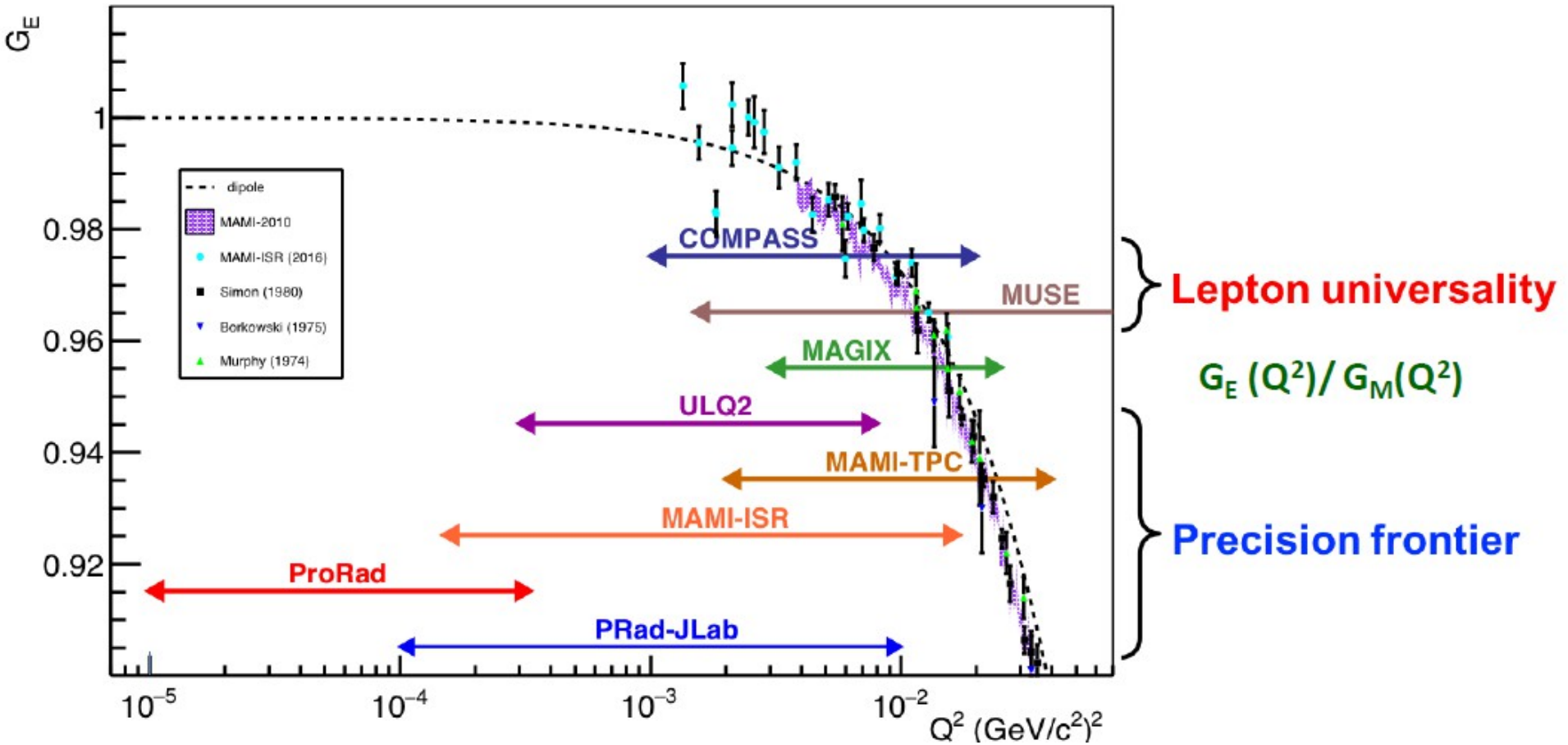

Figure taken from the talk of D. Marchand (PRP 2018)

Backup

The ep elastic scattering cross sections are given by the following expression:

$$\frac{d\sigma}{dt} = \frac{\pi\alpha^2}{t^2}\left\{G_E^2\left[\frac{\left(4M + t/\varepsilon_e\right)^2}{4M^2 - t} + \frac{t}{\varepsilon_e^2}\right] - \frac{t}{4M^2}G_M^2\left[\frac{\left(4M + t/\varepsilon_e\right)^2}{4M^2 - t} - \frac{t}{\varepsilon_e^2}\right]\right\} \quad (1)$$

where $t = -Q^2$, $\alpha = 1/137$, ε_e - initial electron energy, M – proton mass, G_E – electric form factor and G_M – magnetic form factor.

At low Q^2 the form factors can be represented by the expansions:

$$\frac{G\left(Q^2\right)}{G(0)} = 1 - \frac{1}{6}\left\langle R_p^2\right\rangle Q^2 + \frac{1}{120}\left\langle R_p^4\right\rangle Q^4 - \ldots, \quad (2)$$

The electric proton radius R_{pE} can be measured by measuring the slope of the electric form factor G_E as Q^2 goes to 0:

$$R_{pE}^2 = \left.\frac{-6 \cdot dG_E\left(Q^2\right)}{dQ^2}\right|_{Q^2 \to 0} \quad (3)$$

Backup

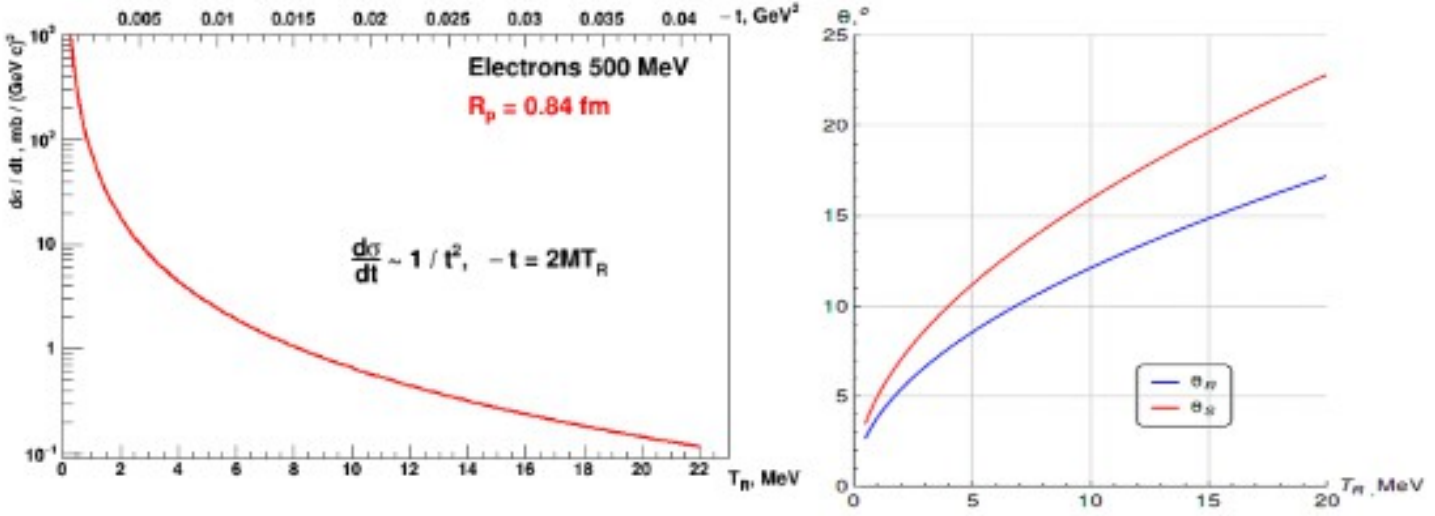

Figure 2: Left panel: differential cross section of the ep elastic scattering calculated for ε = 500 MeV with electric and magnetic form factors represented by expansion Eq. 2. Right panel: Scattering electron and recoil proton angles as function of the recoil proton energy.

The ep elastic scattering differential cross section is given by the following expression:

$$\frac{d\sigma}{dt} = \frac{\pi\alpha^2}{t^2}\left\{G_E^2\left[\frac{(4M + t/\varepsilon)^2}{4M^2 - t} + \frac{t}{\varepsilon^2}\right] - \frac{t}{4M^2}G_M^2\left[\frac{(4M + t/\varepsilon)^2}{4M^2 - t} - \frac{t}{\varepsilon^2}\right]\right\}, \quad (1)$$

where $t = -Q^2$, $\alpha = (137)^{-1}$ – fine structure constant, ε – initial electron energy, M – proton mass, G_E and G_M — proton electric and magnetic form factors. At the low Q^2, the form factors can be represented by the expansions

$$\frac{G_{E,M}(Q^2)}{G_{E,M}(0)} = 1 - \frac{\langle r^2_{pE,M}\rangle}{6}Q^2 + \mathcal{O}(Q^4), \quad (2)$$

Statistics

45 days 33x10^6 events

$$\frac{G(Q^2)}{G(0)} = 1 - \frac{1}{6}\langle R_p^2 \rangle Q^2 + \frac{1}{120}\langle R_p^4 \rangle Q^4 - \ldots,$$

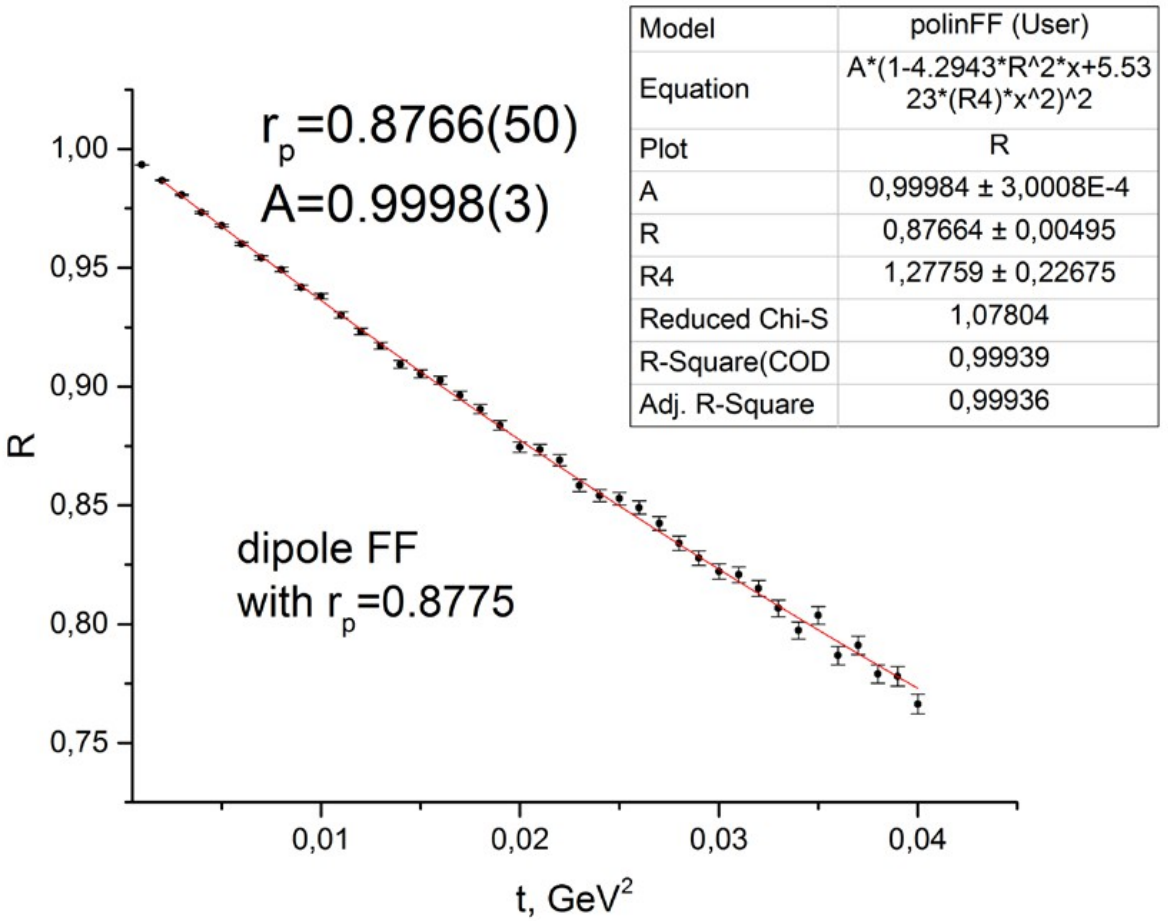

Model	polinFF (User)
Equation	A*(1-4.2943*R^2*x+5.53 23*(R4)*x^2)^2
Plot	R
A	0,99984 ± 3,0008E-4
R	0,87664 ± 0,00495
R4	1,27759 ± 0,22675
Reduced Chi-S	1,07804
R-Square(COD	0,99939
Adj. R-Square	0,99936

Rp ± 0.005 fm

Test setup and beam monitoring system

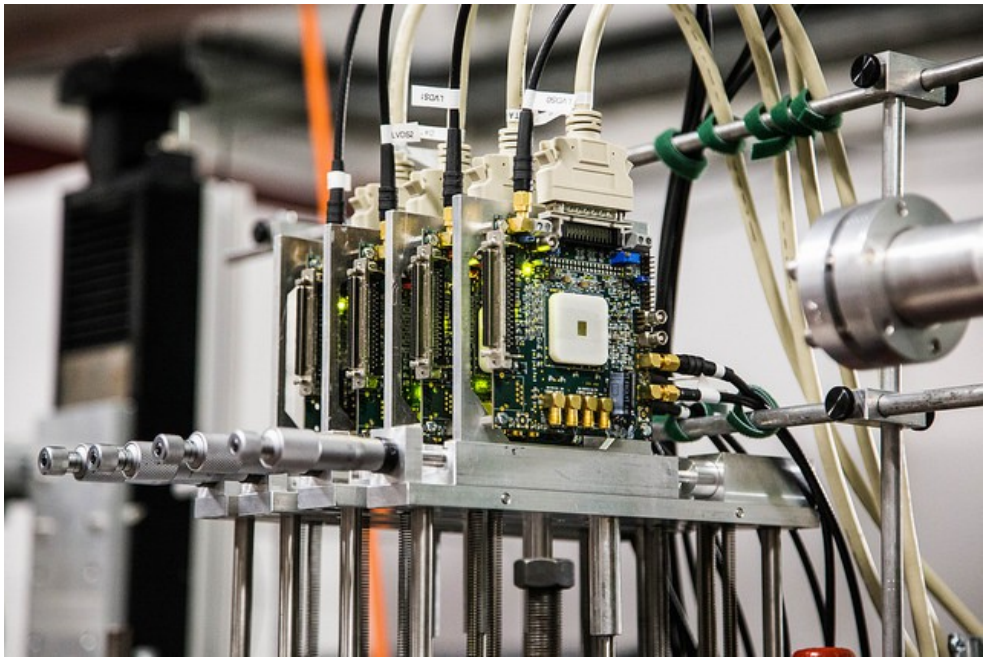

4-layer HV-MAPS pixel detector (3x3 mm)

Monitoring the beam position, reconstruction of electron tracks, and determination of the electron flux

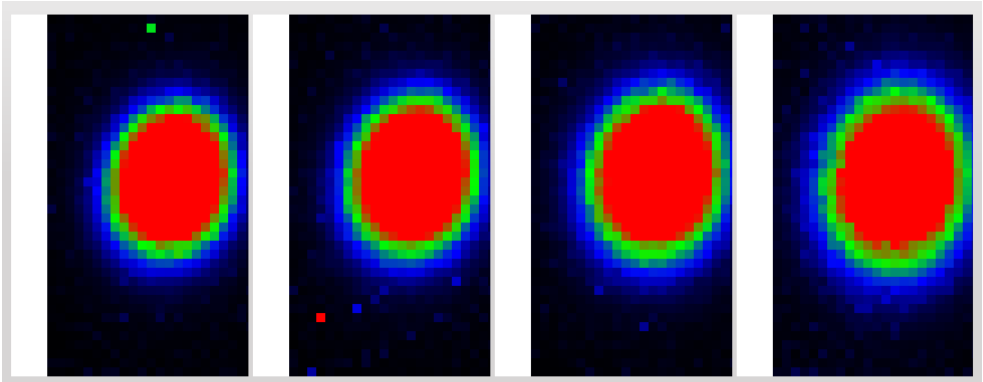

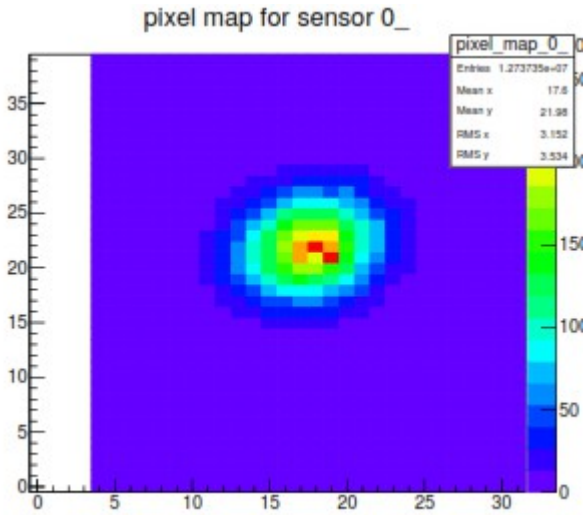

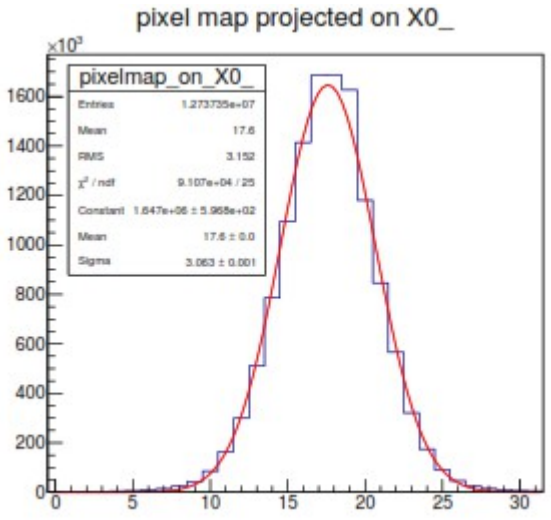

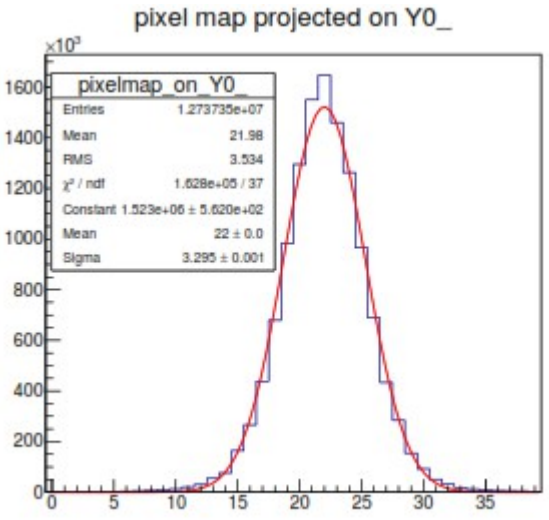

Beam ionization noise in the TPC

Central pad

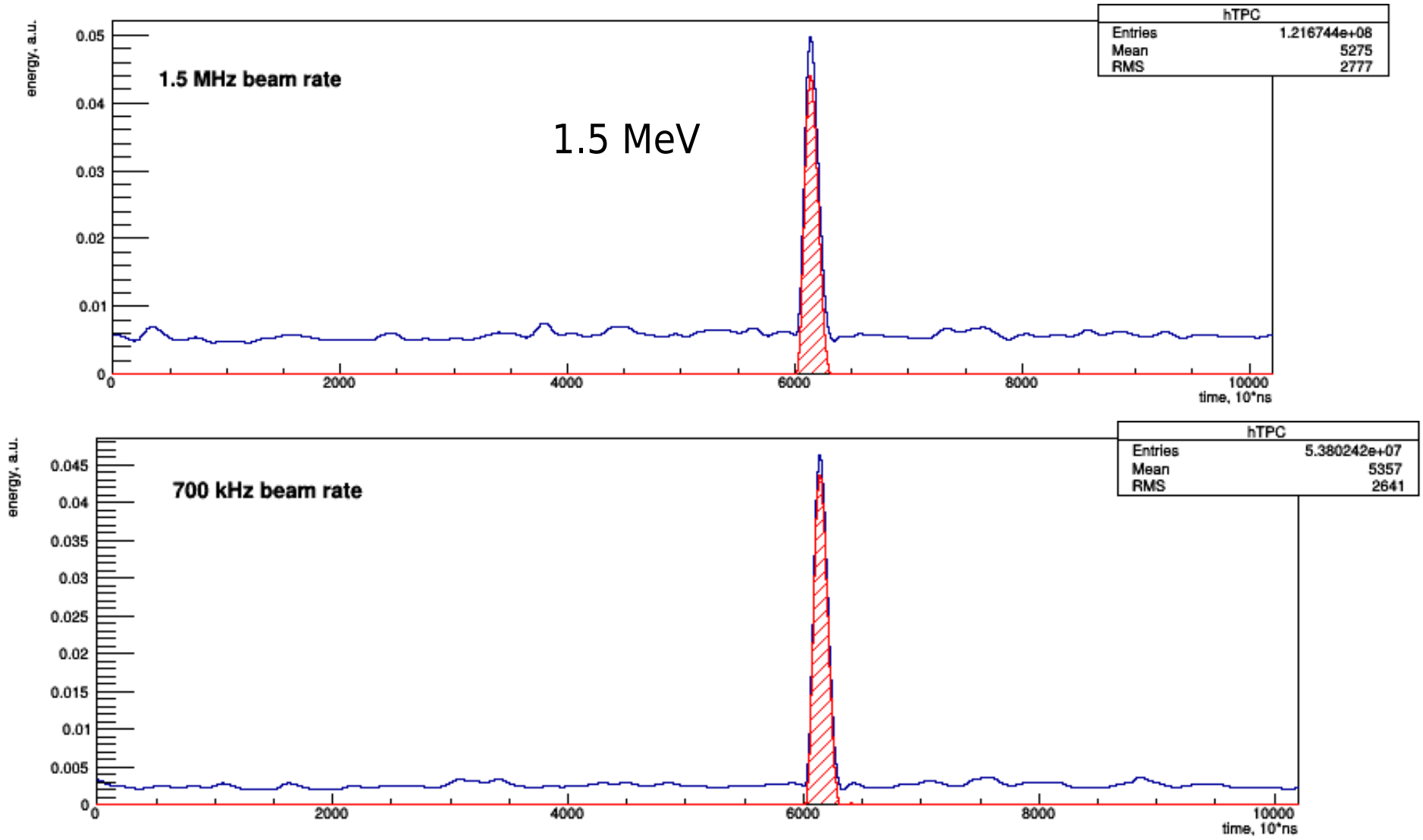

(Alexey Dzyuba, Alexey Vorobyov, PNPI)

Example recoil track in the TPC

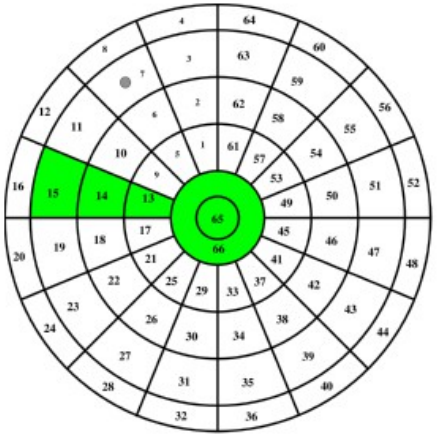

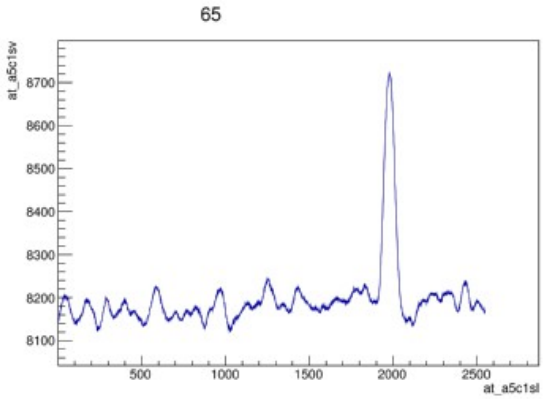

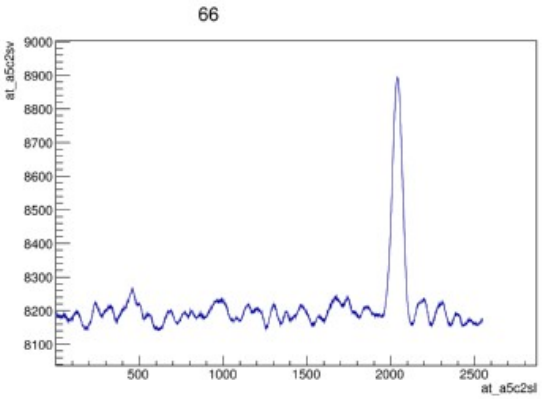

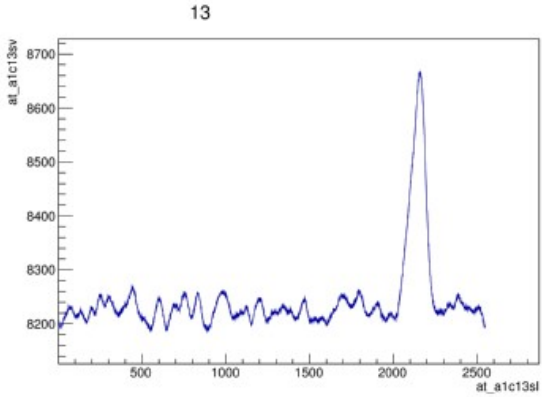

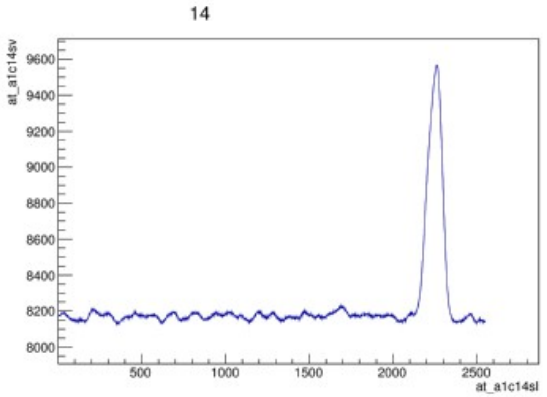

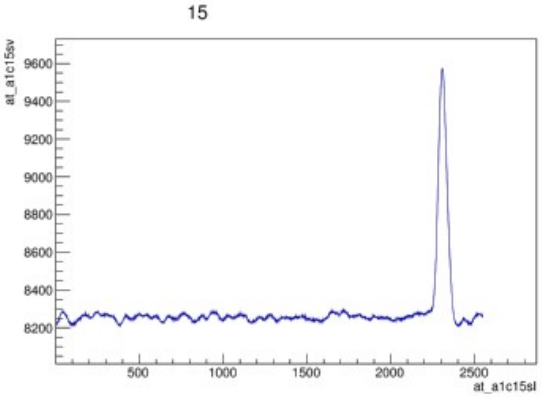

Signals in the TPC clearly identified!

(Alexander Inglessi, PNPI)

Systematic errors

1	Drift velocity, W1	0.01%
2	High Voltage, HV	0.01%
3	Temperature, K	0.015 %
4	Pressure, P	0.01%
5	H_2 density , ρ_p	0.025 %
6	Target length, L_{tag}	0.02 %
7	Number of protons in target, N_p	0.045 %
8	Number of beam electrons, N_e	0.05 %
9	Detection efficiency	0.05 %
10	Electron beam energy, ε_e	0.02 %
11	Electron scattering angle, θ_e	0.02 %
12	t-scale calibration, T_R relative	0.04 %
13	t-scale calibration, T_R absolute	0.08 %
	$d\sigma/dt$, relative	0.1%
	$d\sigma/dt$, absolute	0.2%

$[d\sigma/dt]_{Rp} / [d\sigma/dt]_{Rp=0}$

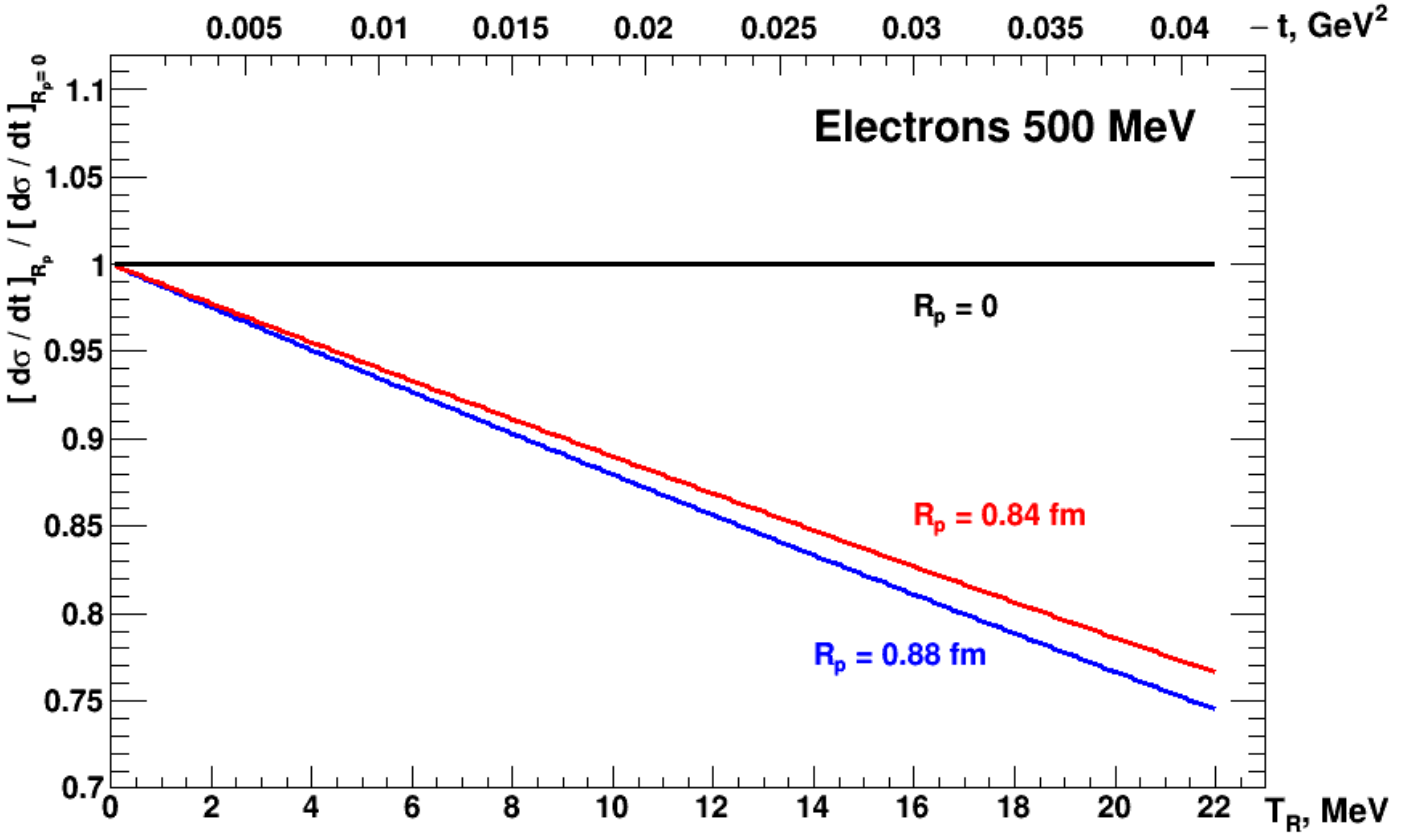

Difference in dσ/dt between Rp=0.84 fm and Rp=0.88 fm is only 1.3% at Q^2 =0.02Gev²

Sensitivity of dσ/dt to proton radius

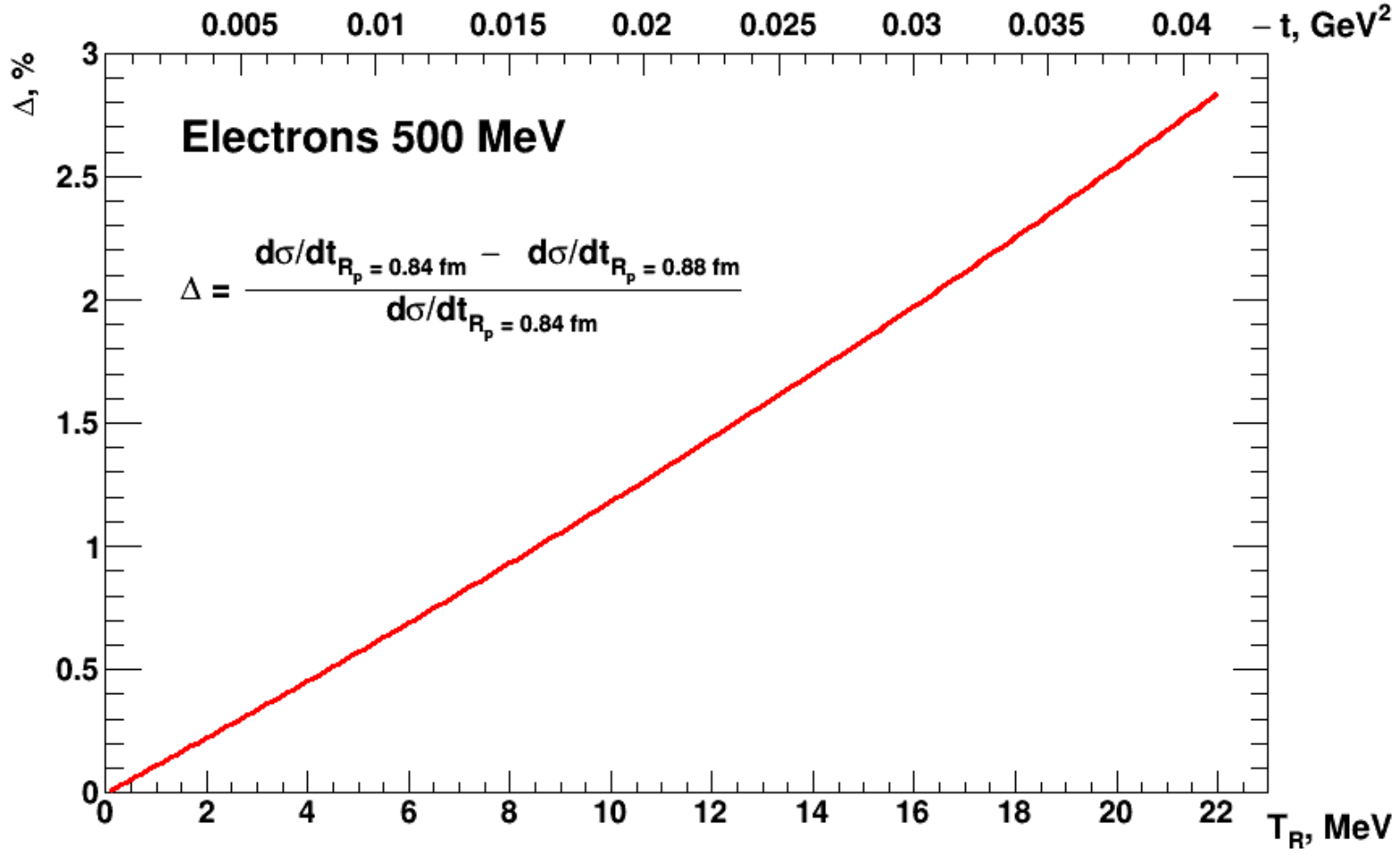

Mesurement of dσ/dt with point-to-point precision 0.1%

Backup

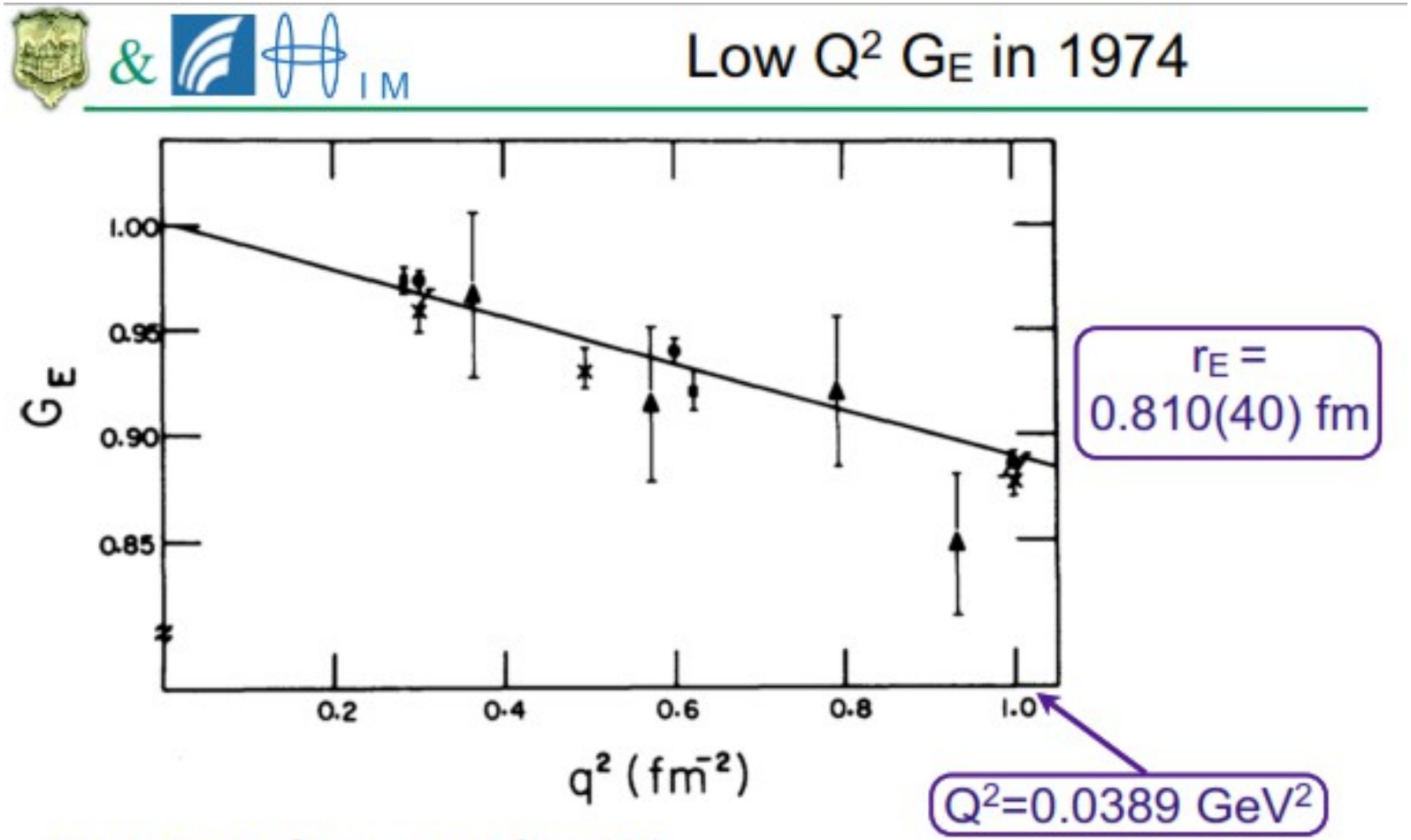

Fit to $G_E(Q^2)=a_0+a_1Q^2+a_2Q^4$
Saskatoon 1974

factor we deduce an rms charge radius for the proton of 0.81 ± 0.04 fm, which is in agreement with the generally accepted value of 0.805 ± 0.011 fm,[5]

Murphy PRC9(74)2125

Backup

The ep elastic scattering cross sections are given by the following expression:

$$\frac{d\sigma}{dt} = \frac{\pi\alpha^2}{t^2}\left\{G_E^2\left[\frac{\left(4M + t/\varepsilon_e\right)^2}{4M^2 - t} + \frac{t}{\varepsilon_e^2}\right] - \frac{t}{4M^2}G_M^2\left[\frac{\left(4M + t/\varepsilon_e\right)^2}{4M^2 - t} - \frac{t}{\varepsilon_e^2}\right]\right\} \quad (1)$$

where $t = -Q^2$, $\alpha = 1/137$, ε_e - initial electron energy, M – proton mass, G_E – electric form factor and G_M – magnetic form factor.

At low Q^2 the form factors can be represented by the expansions:

$$\frac{G\left(Q^2\right)}{G(0)} = 1 - \frac{1}{6}\left\langle R_p^2\right\rangle Q^2 + \frac{1}{120}\left\langle R_p^4\right\rangle Q^4 - \ldots, \quad (2)$$

The electric proton radius R_{pE} can be measured by measuring the slope of the electric form factor G_E as Q^2 goes to 0:

$$R_{pE}^2 = \left.\frac{-6 \cdot dG_E\left(Q^2\right)}{dQ^2}\right|_{Q^2 \to 0} \quad (3)$$

Backup

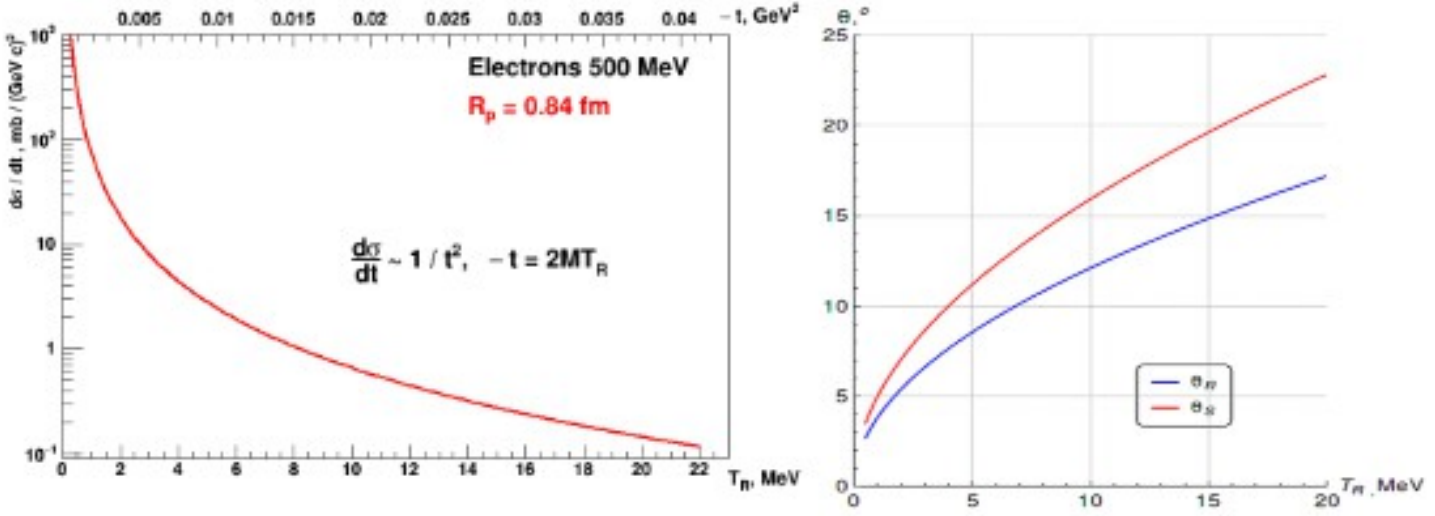

Figure 2: Left panel: differential cross section of the ep elastic scattering calculated for ε = 500 MeV with electric and magnetic form factors represented by expansion Eq. 2. Right panel: Scattering electron and recoil proton angles as function of the recoil proton energy.

The ep elastic scattering differential cross section is given by the following expression:

$$\frac{d\sigma}{dt} = \frac{\pi\alpha^2}{t^2}\left\{G_E^2\left[\frac{(4M + t/\varepsilon)^2}{4M^2 - t} + \frac{t}{\varepsilon^2}\right] - \frac{t}{4M^2}G_M^2\left[\frac{(4M + t/\varepsilon)^2}{4M^2 - t} - \frac{t}{\varepsilon^2}\right]\right\}, \quad (1)$$

where $t = -Q^2$, $\alpha = (137)^{-1}$ – fine structure constant, ε – initial electron energy, M – proton mass, G_E and G_M — proton electric and magnetic form factors. At the low Q^2, the form factors can be represented by the expansions

$$\frac{G_{E,M}(Q^2)}{G_{E,M}(0)} = 1 - \frac{\langle r^2_{pE,M}\rangle}{6}Q^2 + \mathcal{O}(Q^4), \quad (2)$$

Beamline construction

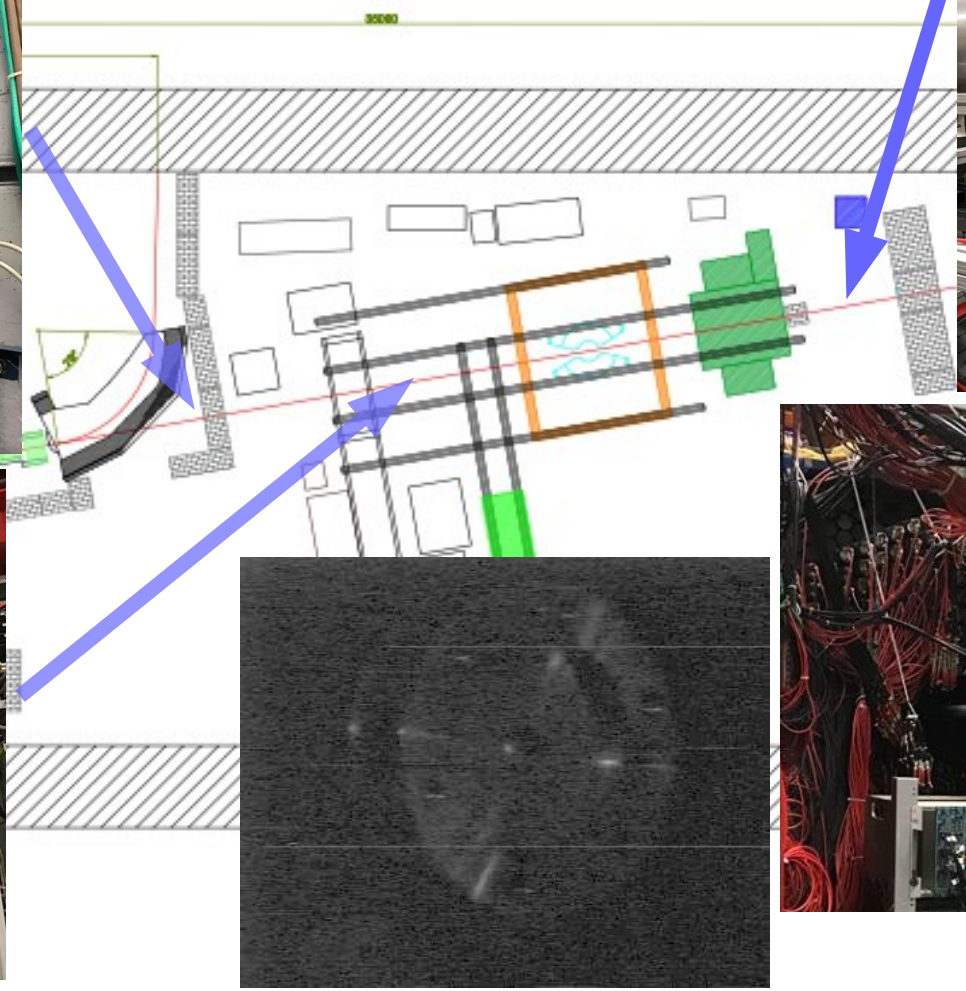

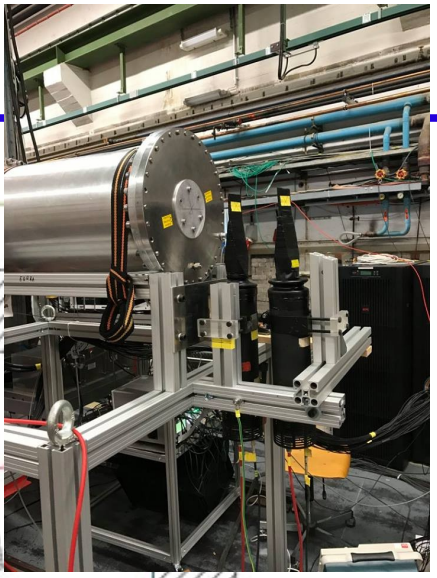

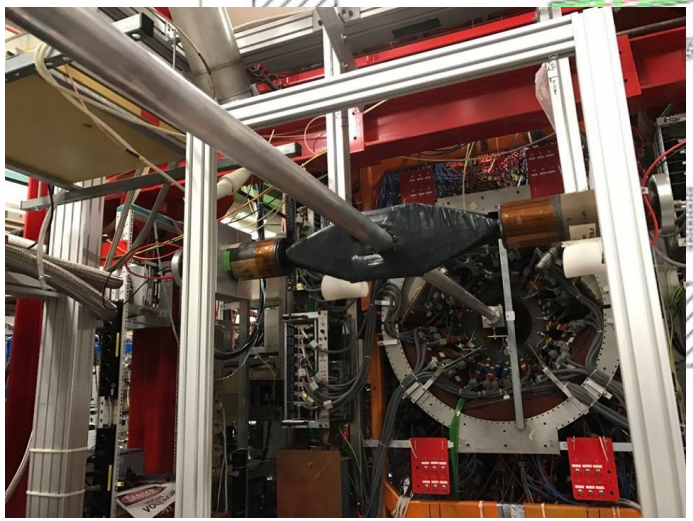

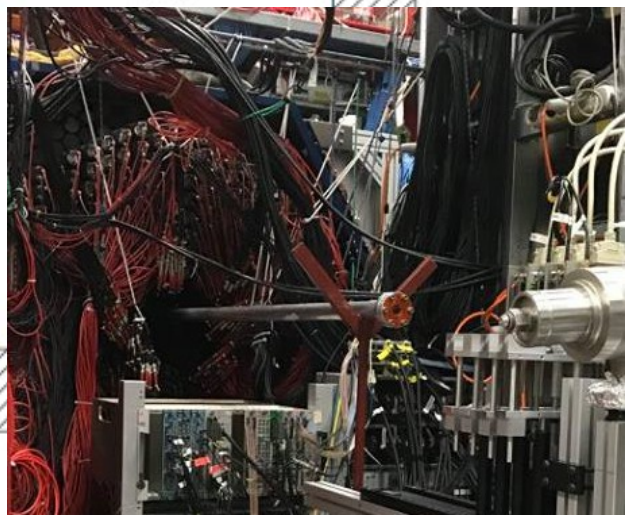

- One horizontal and one vertical steering magnets before tagger wall, luminescent screens for steering, ionization chamber connected to the interlock (M. Dehn)
- Beam scintillators (M. Biroth, O. Kiselev, P. Drexler)
- Beam telescope (F. Wauters, A. Tyukin, M. Zimmermann, N. Berger)
- PIZZA detector (P. Drexler, A. Inglessi, O. Kiselev)
- Scintillator counters before Crystal Ball (M. Biroth)

TPC gas fillings

H_2 4 bar	$T_R \leq 4$ MeV
H_2 20 bar	$T_R \leq 10$ MeV
CH_4	$T_R \leq 22$ MeV

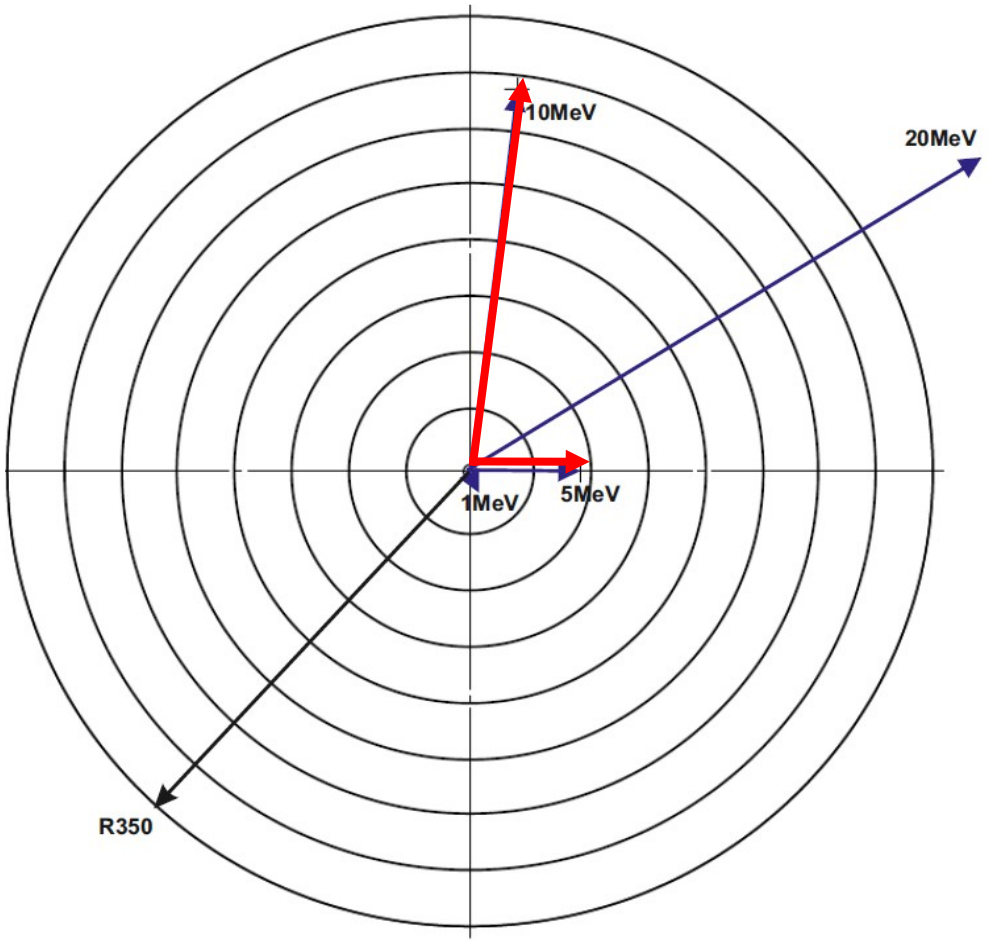

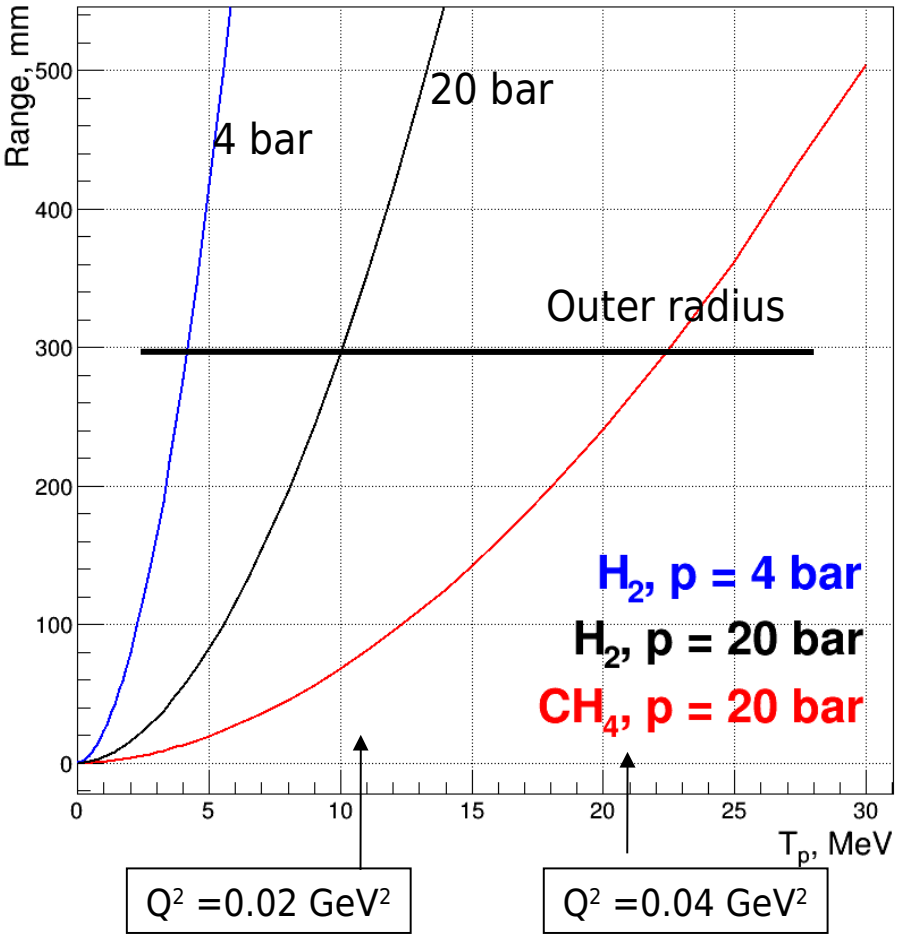

TPC anode structure: 10 mm in diameter disc surrounded by 7 rings

Event selection and background suppression

- Trigger: E_R > 300 keV
- Time coincidence between signals in the TPC and Forward Tracker
- Tracing back the electron trajectory: matching the Z coordinate for the vertex determined from the TPC and Forward Tracker
- Background suppression using various correlations.

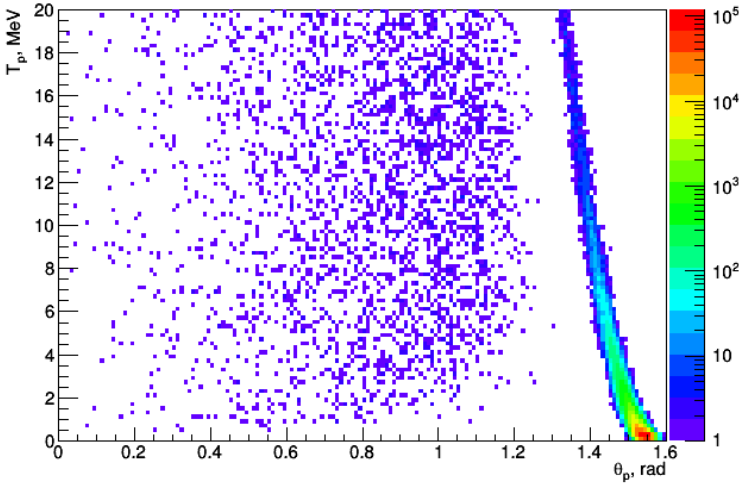

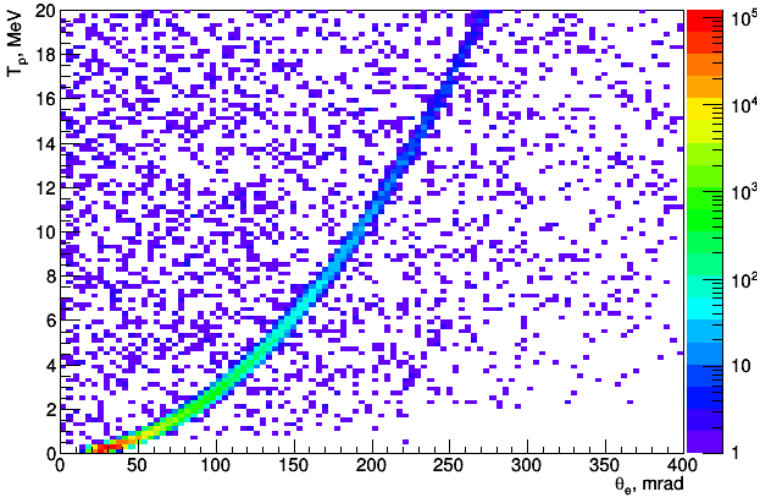

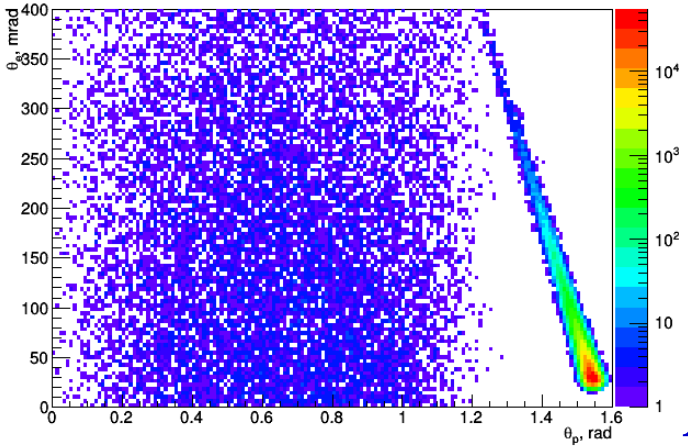

Simulation for the elastic ep scattering and compared with the background reaction $ep \rightarrow ep\pi^0$ for ε_e = 720 MeV

A. Dzyuba, A. Vorobyov (PNPI)

Anode segmentation in ACTAR2

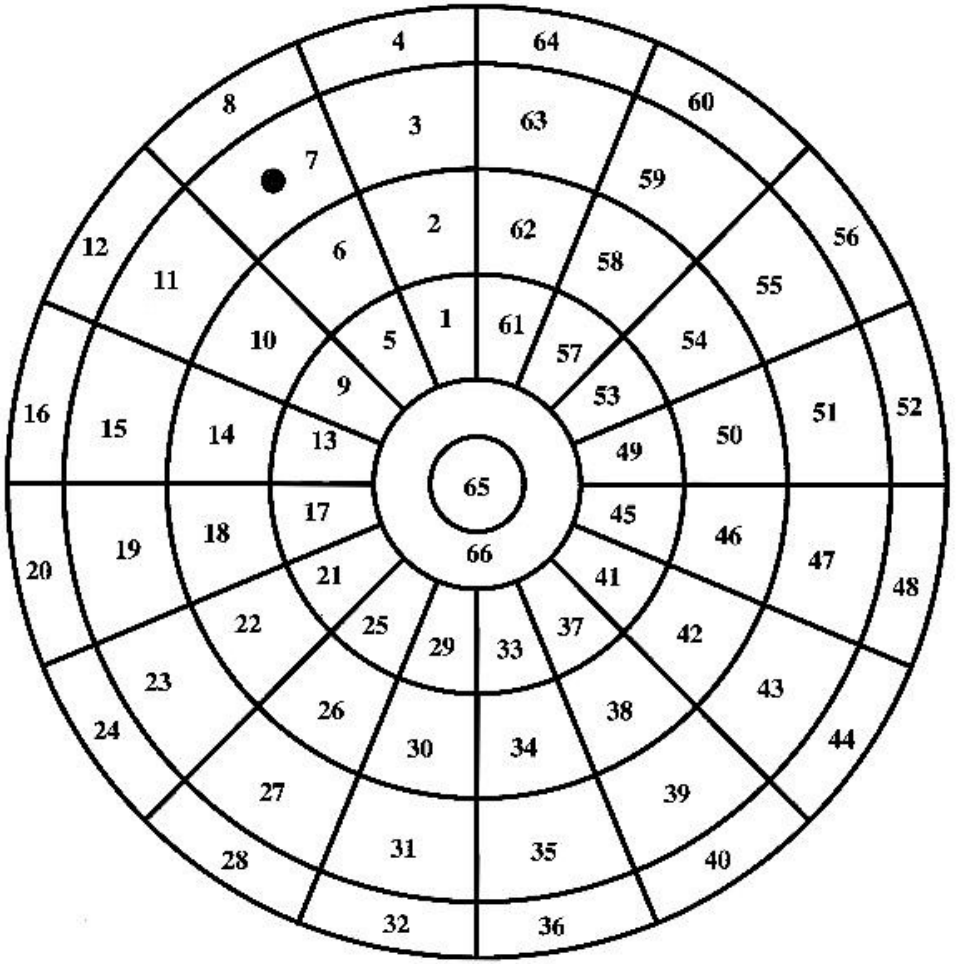

. *66 pads in total. The central pad is 20 mm in diameter*

Read out with FADC from each pad

Radiative corrections

$$\left(\frac{d\sigma}{d\Omega}\right)_1 = \left(\frac{d\sigma}{d\Omega}\right)_0 (1+\delta).$$

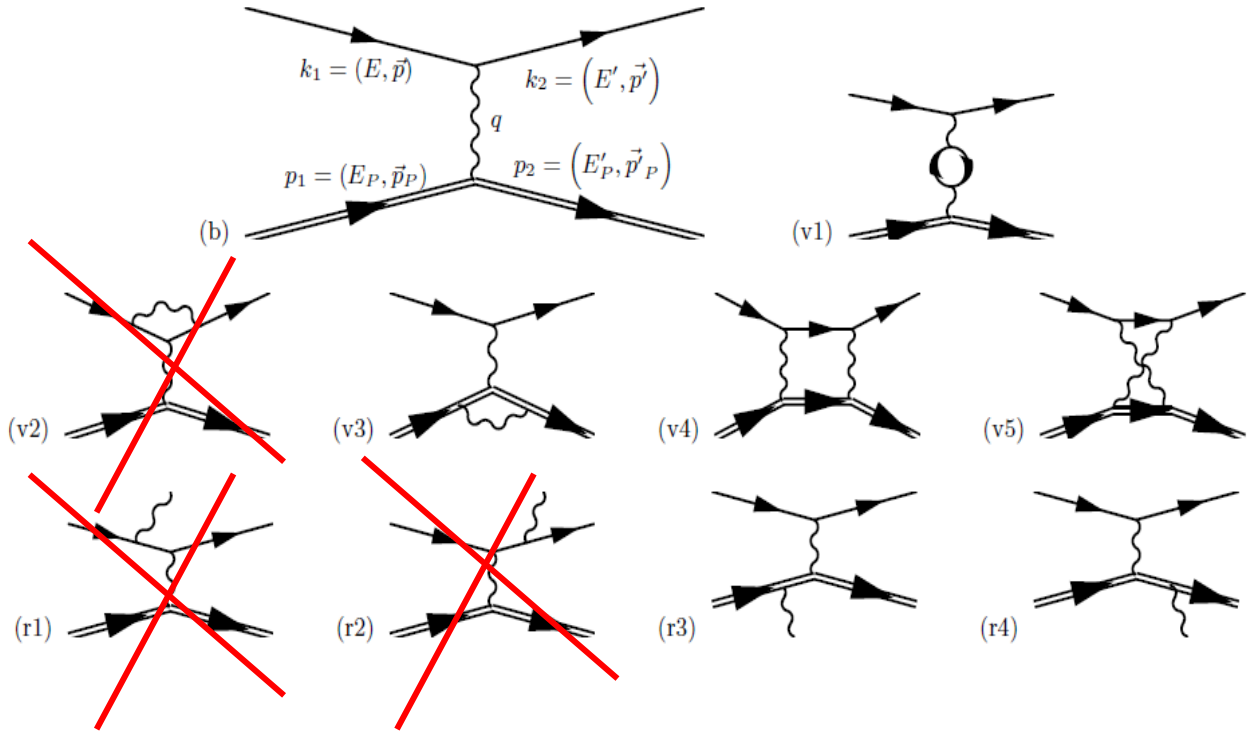

Diagrams v2, r1,r2 are self-cancelling in the recoil method.
The other RC are small and can be calculated to ≤ 0.1% precision.

Absolute measurement of dσ/dt with 0.2% precision
gives a control for the level of introduced radiative corrections.

Vacuum polarization is the largest RC in this method

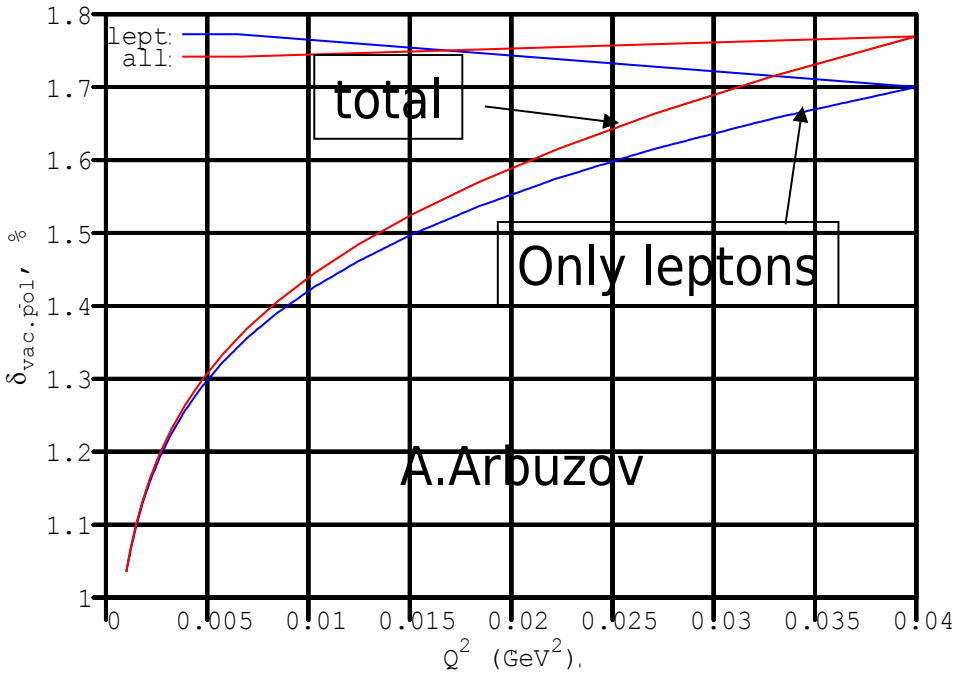

Q^2=0.022 GeV^2
δ_{VP} =1.61546((28)%

The other corrections will be calculated with the Novosibirsk ESEPP generator

Statistics

45 days 33x10^6 events

$$\frac{G(Q^2)}{G(0)} = 1 - \frac{1}{6}\langle R_p^2 \rangle Q^2 + \frac{1}{120}\langle R_p^4 \rangle Q^4 - \ldots,$$

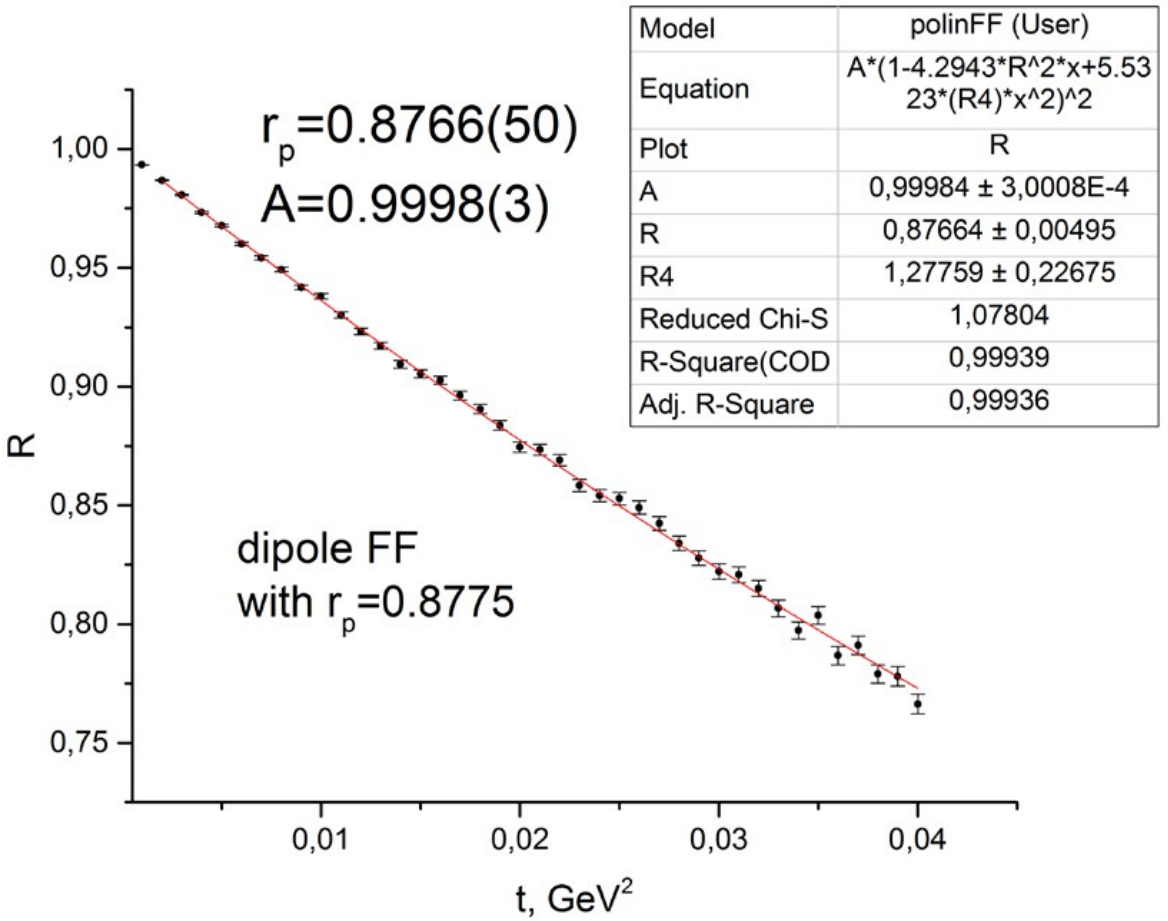

Model	polinFF (User)
Equation	A*(1-4.2943*R^2*x+5.53 23*(R4)*x^2)^2
Plot	R
A	0,99984 ± 3,0008E-4
R	0,87664 ± 0,00495
R4	1,27759 ± 0,22675
Reduced Chi-S	1,07804
R-Square(COD	0,99939
Adj. R-Square	0,99936

Rp ± 0.005 fm

Prototype for the beam monitoring system

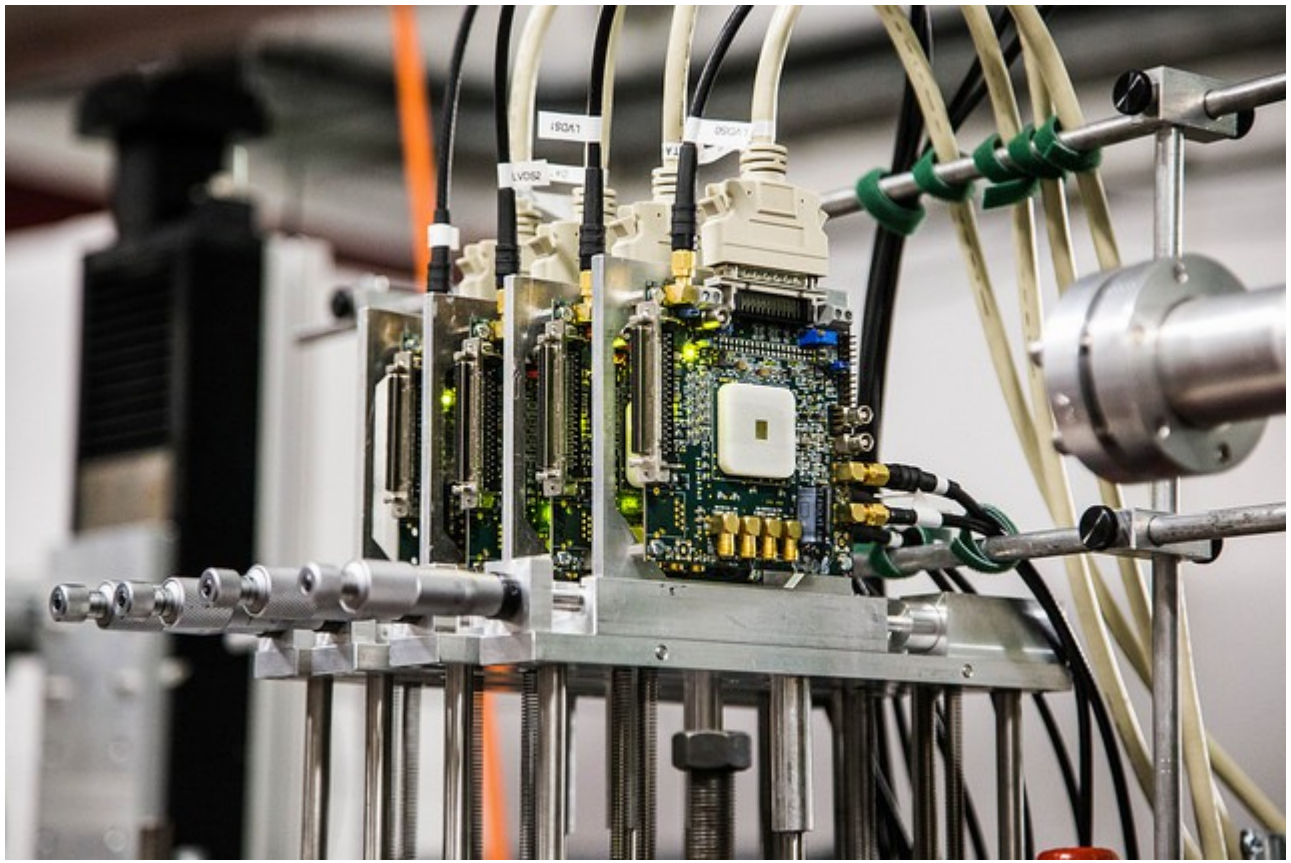

Mupix 7:

- 32 x 40 pixels of 103 um x 80 um
- 62.5 MHz timestaps
- 1.25 Gb/s readout to FPGA
- Track based alignment to better than 5 um
- 99 % efficiency per plane
  (Frederik Wauters, Mainz)

Backup

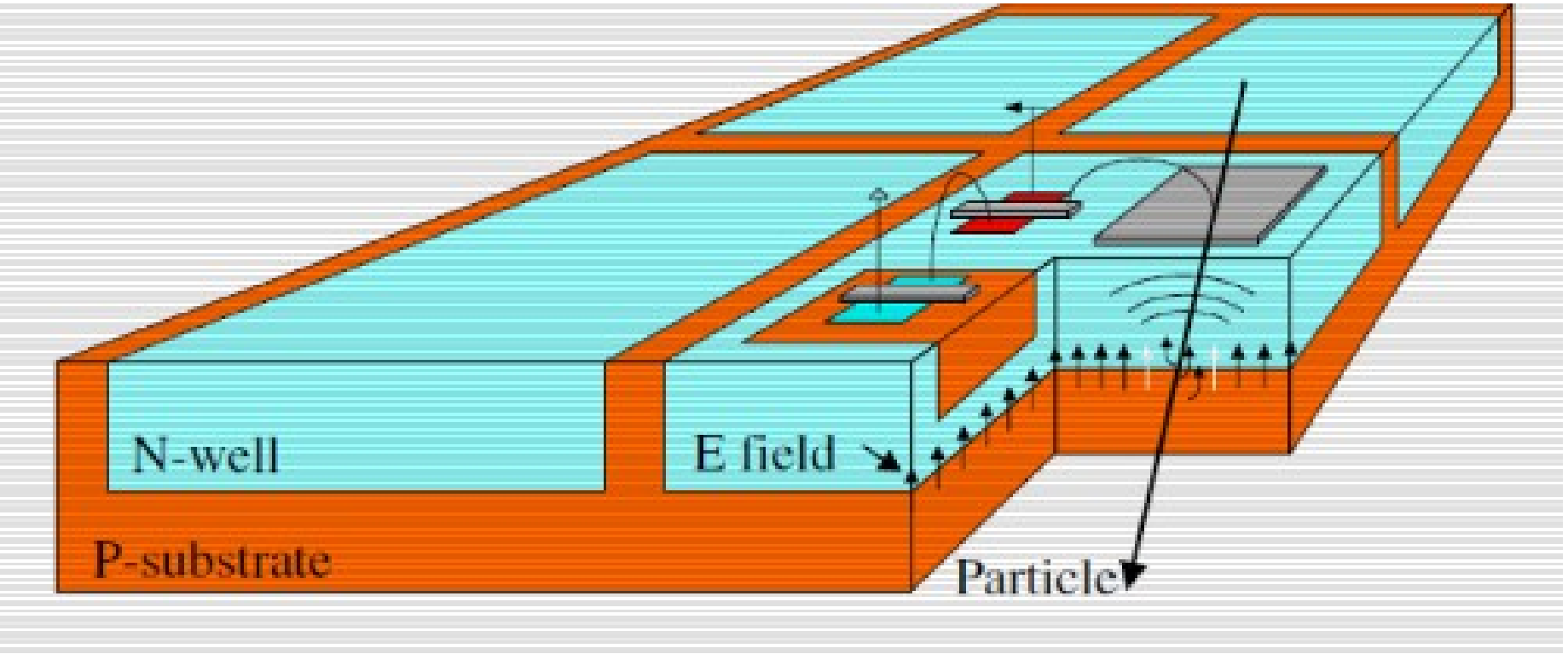

Backup (Patrik Adlarson)

Bethe–Heitler (BH) process

JOHANNES GUTENBERG UNIVERSITÄT MAINZ

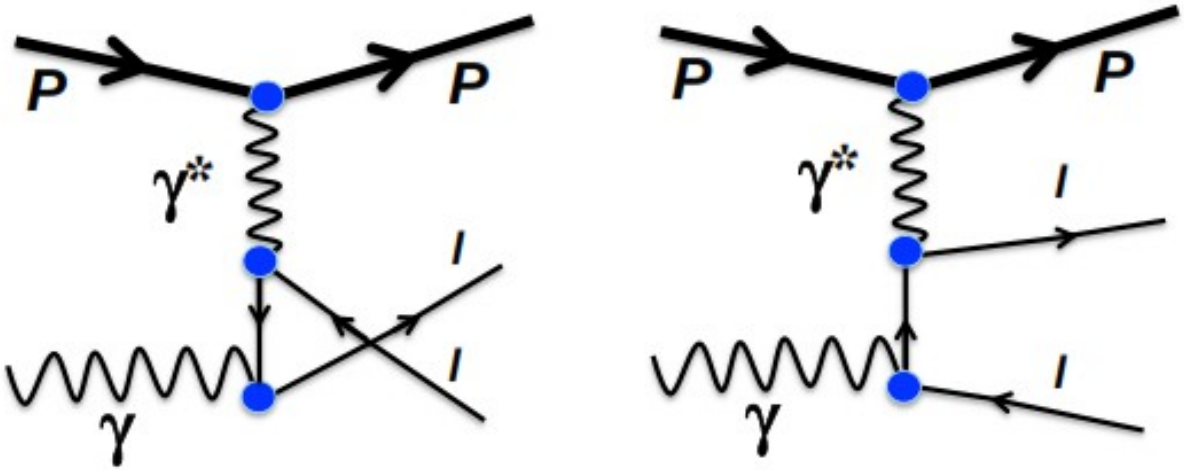

$$\frac{d\sigma^{BH}}{dt dM_{ll}^2} = \frac{\alpha^3}{(s-M_p^2)^2} \cdot \frac{4\beta}{t^2(M_{ll}^2-t)^4} \cdot \frac{1}{1+\tau} \times \left[C_E G_{E_p}^2 + C_M \tau G_{M_p}^2\right]$$

Invariant mass sq lepton pair

Proton mom transfer

Proton form factors

Backup (Patrik Adlarson)

Bethe–Heitler dσ/dEγ

JOHANNES GUTENBERG UNIVERSITÄT MAINZ

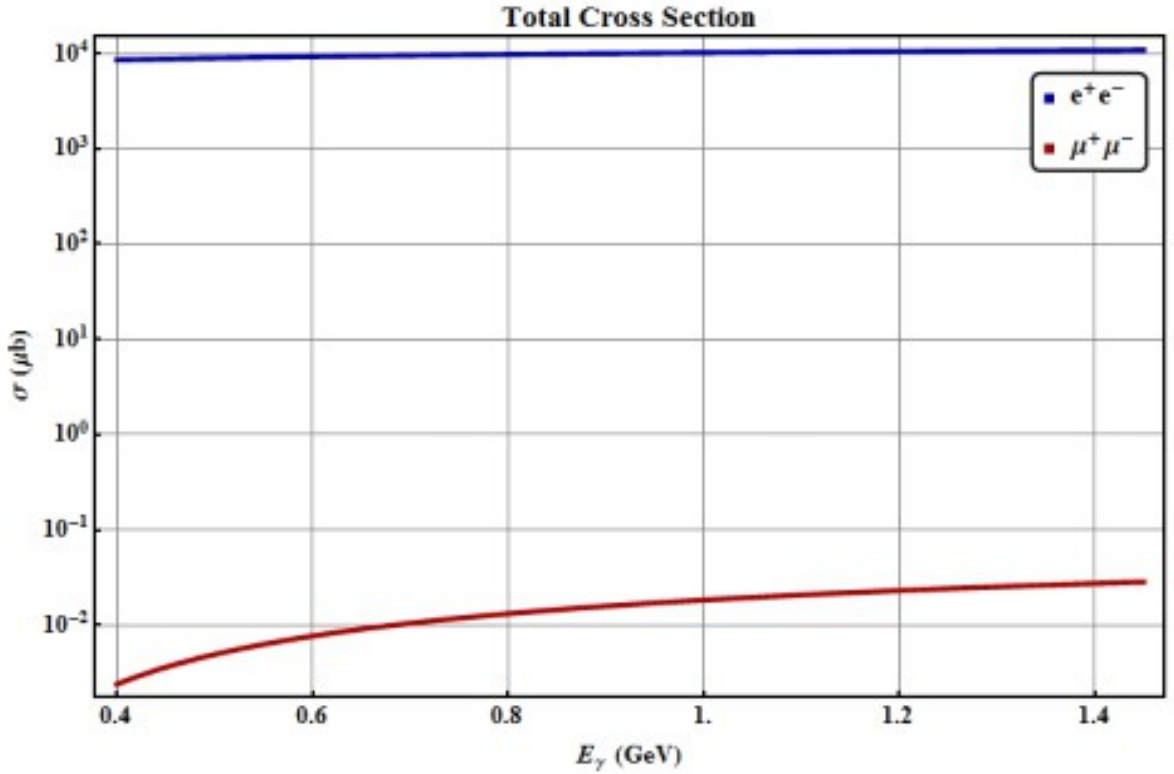

BH-ee (blue) and BH-μμ (red) cross section as function of beam energy

Dimuon cross section increases more for increasing beam energies

Backup

		Syst. Error %	comment
1	Drift velocity, W1	0.01	
2	High Voltage, HV	0.01	
3	Pressure, P	0.01	
4	Temperature, K	0.015	
5	H_2 density , ρ_p	0.025	Sum of errors 3 and 4
6	Target length, L_{targ}	0.02	
7	Number of protons in target, N_p	0.045	Sum of errors 5 and 6
8	Number of beam electrons, N_e	0.05	
9	Detection efficiency	0.05	
10	Electron beam energy, ε_e	0.02	
11	Electron scattering angle, θ_e	0.02	
12	t-scale calibration, T_R relative	0.04	Follows from error 11
13	t-scale calibration, T_R absolute	0.08	Follows from the sum of errors 11 and 10
	$d\sigma/dt$, relative	0.1	0.08 % from error 12
	$d\sigma/dt$, absolute	0.2	0.16 % from err.13 plus errors 7,8, and 9

A. Vorobyov (PNPI)

Backup

MAMI Specifications

Beam energy	500 MeV, 720 MeV
Energy spread	< 20 keV (1σ)
Energy shift	< 20 keV (1σ)
Absolute energy	±< 150 keV (1 σ)

Electron Beam Specifications

Beam intensity (main run)	2x10^6 e^-/sec
Beam intensity for calibration	10^4 e^-/sec and 10^3 e^-/sec
Beam divergency	≤ 0.5 mrad
Beam size	minimal at given divergence

Beam Time Request

Test run in 2017	~ 2 weeks
First physics run in 2018	~ one month

A. Vorobyov (PNPI)

Crystal Ball/TAPS (slide taken from M. Unverzagt)

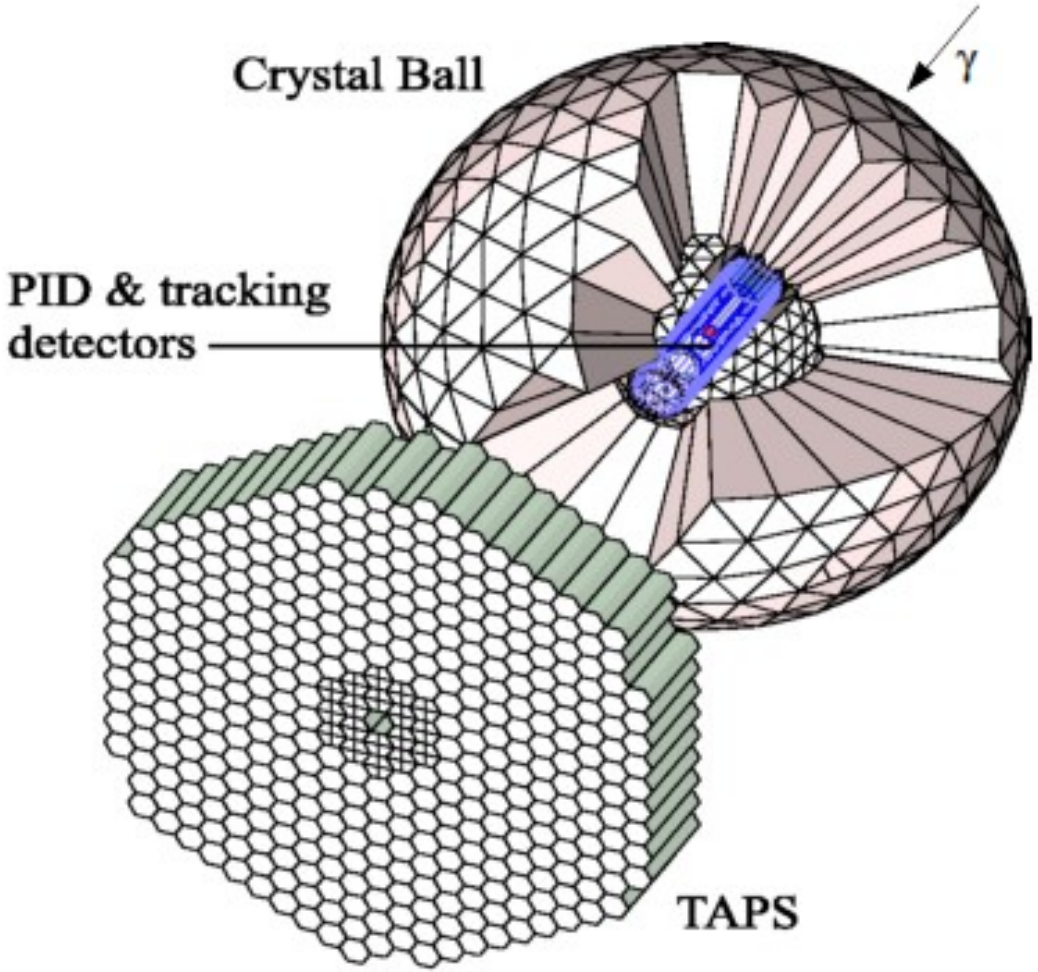

Crystal Ball:
672 NaI(Tl) crystals
93,3% of total solid angle
Each crystal equipped with PMT

$$\frac{\sigma}{E_\gamma} = \frac{2\%}{(E_\gamma/GeV)^{0.25}}$$

Δt = 2.5 ns FWHM

$$\sigma(\theta) = 2^\circ \ldots 3^\circ$$

$$\sigma(\phi) = \frac{2^\circ \ldots 3^\circ}{\sin(\theta)}$$

TAPS:
Up to 510 BaF_2 crystals
Polar acceptance: 4-20°

Δt = 0.5 ns FWHM

$$\frac{\sigma}{E_\gamma} = \frac{0{,}79\%}{\sqrt{E_\gamma/GeV}} + 1{,}8\%$$

Measurement of α and β

$$\Sigma_3 = \Sigma_3^{(\mathrm{B})} - \frac{4M\omega^2 \cos\theta \sin^2\theta}{\alpha_{em}(1+\cos^2\theta)^2}\,\beta_{M1} + O(\omega^4), \quad (6)$$

where $\Sigma_3^{(\mathrm{B})}$ is the pure Born contribution, while

$$\omega = \frac{s - M^2 + \frac{1}{2}t}{\sqrt{4M^2 - t}}, \quad \theta = \arccos\left(1 + \frac{t}{2\omega^2}\right) \quad (7)$$

are the photon energy and scattering angle in the Breit (brick-wall) reference frame. In fact, to this order in the LEX the formula is valid for ω and θ being the energy and angle in the lab or center-of-mass frame.

N. Krupina and V. Pascalutsa [PRL 110, 262001 (2013)]

Measurement of α and β

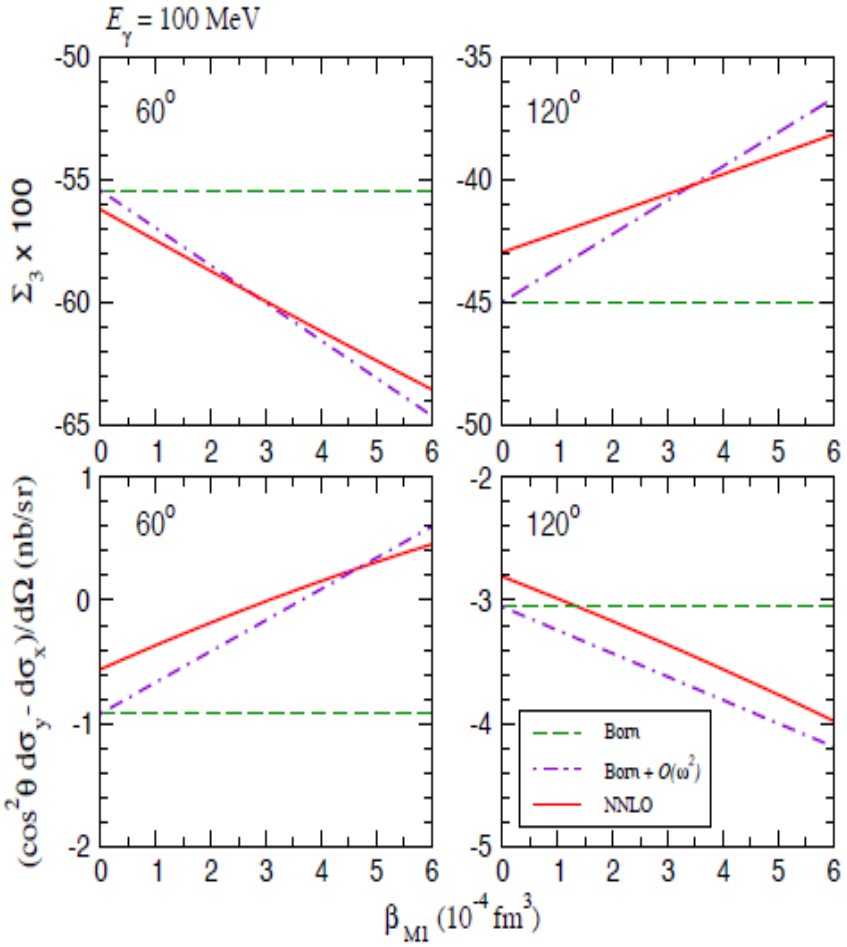

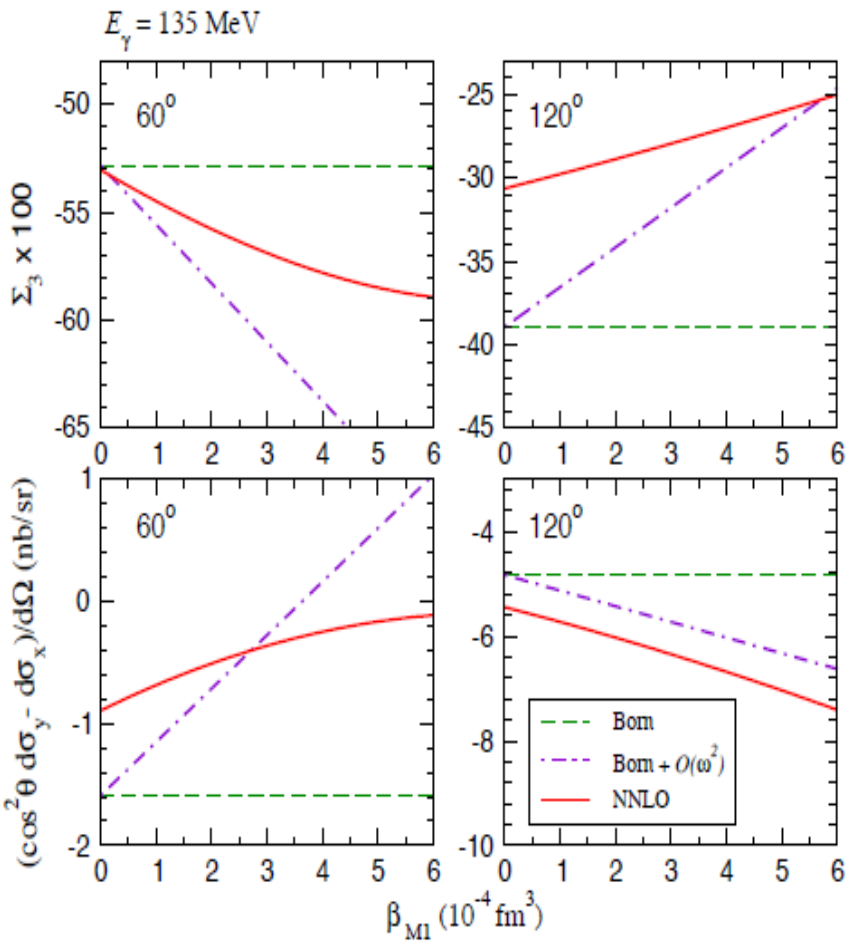

IKAR-M detector

New-generation experiments with a completely different systematics:

- Electron scattering with detection of both recoil proton and scattered electron
- Dilepton photoproduction (proton radius measurement, lepton universality test)

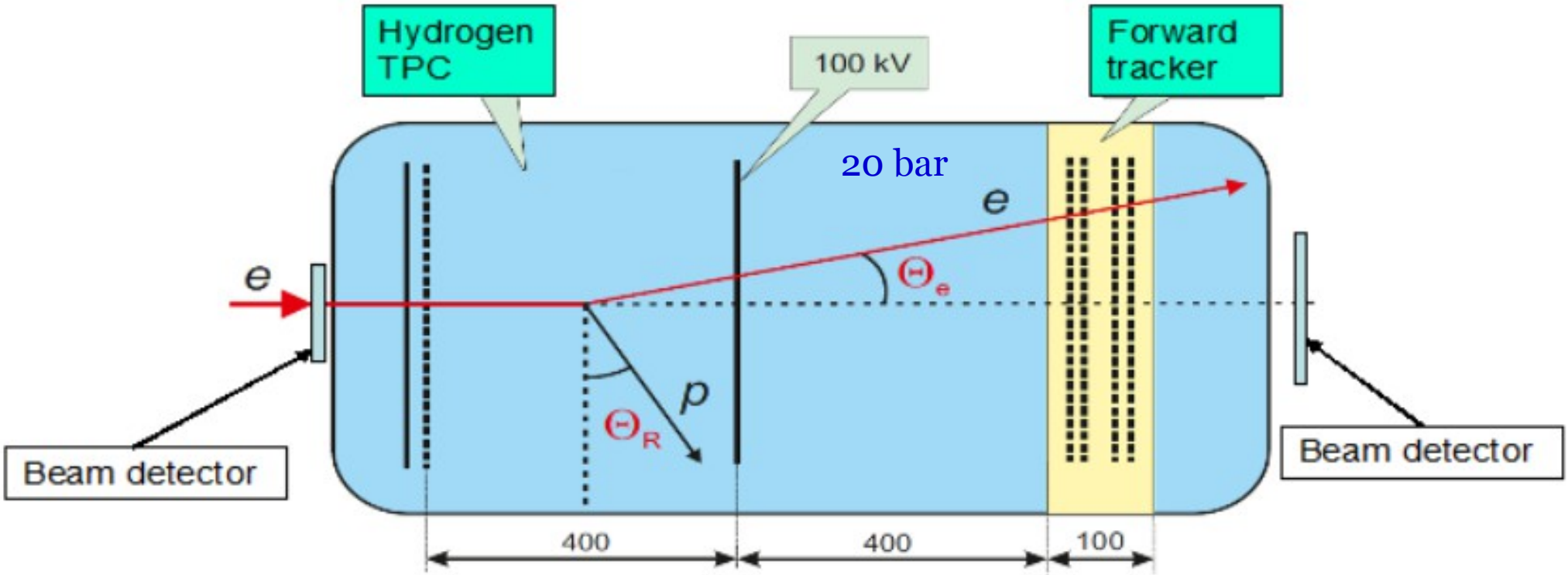

TPC&FT at MAMI beam will open avenue for various experiments:

- Experiments with electron and photon beams in A2 with accurate detection of charged particles (including recoil fragments)
- Hydrogen, deuterium, helium gas filling possible
- Longer term: transfer of technology to experiments at MESA accelerator e.g. for complementary measurement of the nucleon scalar polarizabilities (in addition to the A2 program)

IKAR-M detector

New-generation experiments with a completely different systematics:

- Electron scattering with detection of both recoil proton and scattered electron
- Dilepton photoproduction (proton radius measurement, lepton universality test)

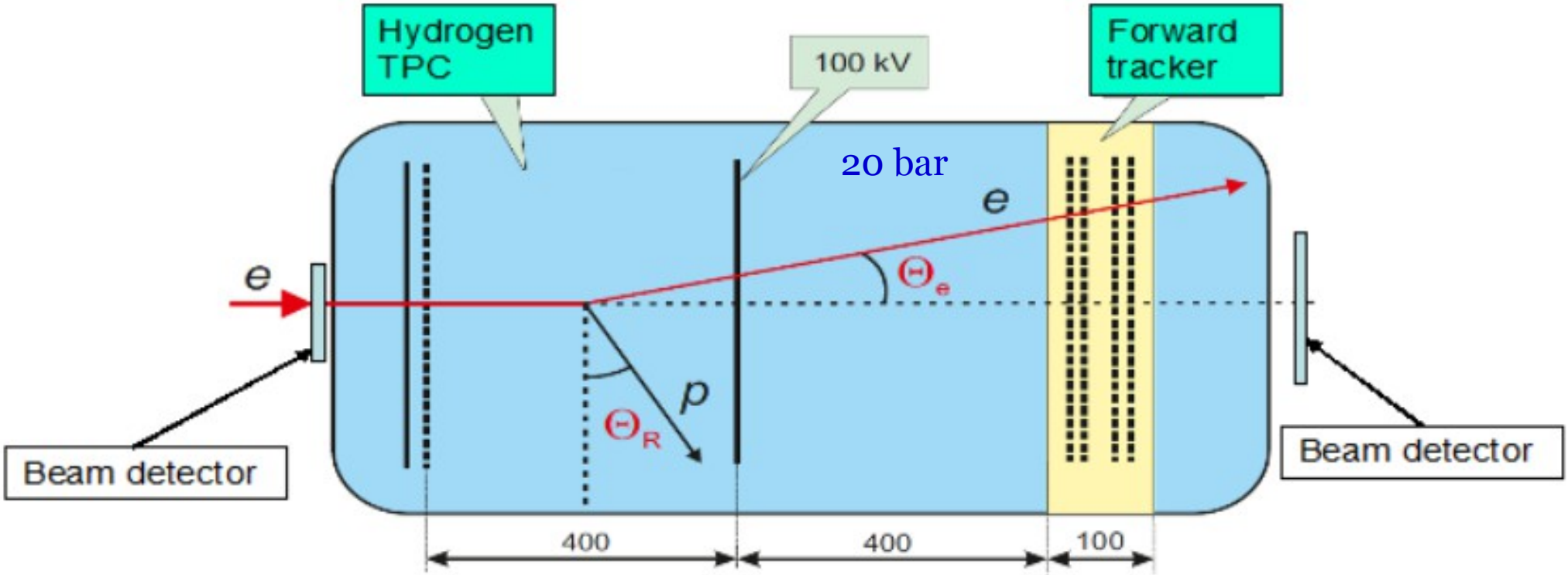

Measured quantities:

Recoil energy T_R

Recoil angle Θ_R

Vertex Z coordinate

E scattering angle Θ_e

$$-t = \frac{4\varepsilon_e^2 \sin^2\frac{\vartheta}{2}}{1+\frac{2\varepsilon_e}{M}\sin^2\frac{\vartheta}{2}}$$

$$-t = 2MT_R$$

Gas pressure (bar)	4, 20
Drift distance, (mm)	300± 0.1
σ_z (μm)	150
σ_{T_p} (keV)	60
σ_{θ_p} (mrad)	10-15
$\sigma_{x/y/z}$ tracker (z TPC) (μm)	30/30/150
σ_t TPC/ tracker (ns)	40/5
θ_{max} (°)	32